



# Genes critical for development and differentiation of dopaminergic neurons are downregulated in Parkinson's disease

Aditi Verma, Reddy Peera Kommaddi, Barathan Gnanabharathi, Etienne Hirsch, Vijayalakshmi Ravindranath

## ► To cite this version:

Aditi Verma, Reddy Peera Kommaddi, Barathan Gnanabharathi, Etienne Hirsch, Vijayalakshmi Ravindranath. Genes critical for development and differentiation of dopaminergic neurons are downregulated in Parkinson's disease. Journal of Neural Transmission, 2023, 130 (4), pp.495-512. 10.1007/s00702-023-02604-x . inserm-04002894

HAL Id: inserm-04002894

<https://inserm.hal.science/inserm-04002894>

Submitted on 12 Apr 2023

**HAL** is a multi-disciplinary open access archive for the deposit and dissemination of scientific research documents, whether they are published or not. The documents may come from teaching and research institutions in France or abroad, or from public or private research centers.

L'archive ouverte pluridisciplinaire **HAL**, est destinée au dépôt et à la diffusion de documents scientifiques de niveau recherche, publiés ou non, émanant des établissements d'enseignement et de recherche français ou étrangers, des laboratoires publics ou privés.

# **Genes critical for development and differentiation of dopaminergic neurons are downregulated in Parkinson's disease**

Aditi Verma<sup>1</sup>, Reddy Peera Kommaddi<sup>2</sup>, Barathan Gnanabharathi<sup>2</sup>, Etienne C. Hirsch<sup>3</sup>,

Vijayalakshmi Ravindranath<sup>1,2 \*</sup>

<sup>1</sup> Centre for Neuroscience, Indian Institute of Science, Bangalore-560012, India

<sup>2</sup> Centre for Brain Research, Indian Institute of Science, Bangalore-560012, India

<sup>3</sup> Sorbonne Université, Institut du Cerveau – ICM, Inserm U 1127, CNRS UMR 7225, F-75013, Paris, France

Address for correspondence:  
Vijayalakshmi Ravindranath,  
Centre for Brain Research,  
Indian Institute of Science,  
C.V. Raman Avenue,  
Bangalore - 560012, India.  
Phone: +91-80-22933640  
Fax: +91-80-23607766  
email: [viji@iisc.ac.in](mailto:viji@iisc.ac.in)

**Keywords:** Substantia nigra; RNA-seq; LMX1B; SH-SY5Y; neurodegeneration

**Competing interest statement:** The authors declare that there are no competing interests.

**Running Title:** Midbrain developmental genes in PD

## **Abstract**

We performed transcriptome analysis using RNA sequencing on substantia nigra pars compacta (SNpc) from mice after acute and chronic 1-methyl-4-phenyl-1,2,3,6-tetrahydropyridine (MPTP) treatment and Parkinson's disease (PD) patients. Acute and chronic exposure to MPTP resulted in decreased expression of genes involved in sodium channel regulation. However, upregulation of pro-inflammatory pathways was seen after single dose but not after chronic MPTP treatment. Dopamine biosynthesis and synaptic vesicle recycling pathways were downregulated in PD patients and after chronic MPTP treatment in mice. Genes essential for midbrain development and determination of dopaminergic phenotype such as, *LMX1B*, *FOXA1*, *RSPO2*, *KLHL1*, *EBF3*, *PITX3*, *RGS4*, *ALDH1A1*, *RET*, *FOXA2*, *EN1*, *DLK1*, *GFRA1*, *LMX1A*, *NR4A2*, *GAP43*, *SNCA*, *PBX1*, and *GRB10* were downregulated in human PD and overexpression of GFP tagged *LMX1B* rescued MPP<sup>+</sup> induced death in SH-SY5Y neurons. Downregulation of gene ensemble involved in development and differentiation of dopaminergic neurons indicate their potential involvement in pathogenesis and progression of human PD.

## Introduction

Parkinson's disease (PD) is a debilitating neurodegenerative movement disorder. The cardinal clinical symptoms of PD include rigidity, bradykinesia and resting tremor. PD is characterized by the loss of dopaminergic neurons in the substantia nigra pars compacta (SNpc). While it has been more than 200 years since PD was first characterized by James Parkinson (Parkinson 1817), lack of thorough understanding of the mechanisms that underlie disease pathogenesis has been a major obstacle in discovery of curative treatment modalities. Levodopa administration has been the mainstay for symptomatic treatment for almost sixty years (Cotzias 1968; Hornykiewicz 2010), we do not, as yet, have a disease modifying therapy that can slow down disease progression.

Familial PD is seen in less than 10% of cases, the majority are sporadic (Ascherio and Schwarzschild 2016). The etiology of both familial and sporadic PD is not yet clearly understood, and it is considered to be a complex, multifactorial disorder. Several risk factors have been implicated including oxidative stress, mitochondrial (Schapira et al. 1990; Park et al. 2009) and proteasomal dysfunction (Sherman and Goldberg 2001; Carvalho et al. 2013),  $\alpha$ -synuclein aggregation (Stefanis 2012), neuroinflammation (Hirsch et al. 2012), dopamine metabolism (Pifl et al. 2014) and iron accumulation (Sofic et al. 1988; Ayton and Lei 2014). However, the exact cause underlying PD pathogenesis remain poorly understood. Therefore, understanding the mechanisms that lead to neurodegeneration of dopaminergic neurons in SNpc is vital.

Transcriptomics is a powerful technique that can help investigate all the genes and pathways that might be dysregulated in PD simultaneously. It allows us to identify

dynamic changes in gene expression between different physiological states. Global gene expression analysis using microarray has been deployed to identify critical changes in gene expression in PD (Borrageiro et al. 2018). Many pathways, such as mitochondrial electron transport system, ubiquitin-proteasome system, apoptosis, actin cytoskeleton, inflammation and synaptic transmission have been reported to be dysregulated in PD studies (Zhang et al. 2005; Miller and Federoff 2005; Simunovic et al. 2009; Sutherland et al. 2009; Greene 2012). However, microarray lacks the sensitivity to detect genes which are expressed in low levels, that is they have limited dynamic range of detection (Malone and Oliver 2011; Kogenaru et al. 2012). Moreover, there is low signal to noise ratio as well as there is an upper limit to detection of transcripts beyond which the signal gets saturated. More recently approaches using RNA sequencing (RNA-seq) offer good alternative to examine global gene expression changes in disease state. Several PD studies have employed the RNA-seq technique to understand gene expression changes in the MPTP mouse model (Yang et al. 2021; Tong et al. 2022; Guo et al. 2022), patient brain regions (Keo et al. 2020; Aguila et al. 2021; Tiklová et al. 2021), blood from PD patients (Soreq et al. 2015; Infante et al. 2016; Moni et al. 2019), and iPSCs derived from PD patients (Booth et al. 2019; van den Hurk et al. 2022).

Here, we used RNA seq to identify global gene expression changes in the mouse model of PD following single and chronic exposure to MPTP. Further, RNA-seq was performed to study gene expression alterations in SNpc from human PD patients compared with age-matched controls in an unbiased approach.

## **Materials and Methods**

Animals and MPTP dosing: C57BL/6J male mice (3-4 months; 25-30 grams; RRID:IMSR\_JAX:000664), procured from Central animal facility of Indian Institute of Science were used for all animal experiments. All the animal experiments were designed and followed in compliance with the Animal Research: Reporting of In Vivo Experiments (ARRIVE) guidelines. Animals were housed in groups of five and had access to pelleted diet and water, *ad libitum*. For 1-methyl-4-phenyl-1,2,3,6-tetrahydropyridine hydrochloride (MPTP) mouse model of dopaminergic loss (Jackson-Lewis and Przedborski 2007), MPTP (Sigma-Aldrich Cat. No. M0896) dissolved in normal saline was given at a dose of 30 mg/kg body weight sub-cutaneously to mice as a single injection or daily for 14 days. MPTP injections were carried out in an isolated clean air room in the Central Animal Facility, Indian Institute of Science, Bangalore. Adequate safety precautions were taken for proper handling of MPTP during preparation and injection and for disposal of materials and samples contaminated with MPTP. The controls were injected with an equivalent volume of normal saline. Animals were sacrificed 24 hours after the last MPTP dose.

Preparation of brain coronal sections for histochemical analysis: After 14 days of MPTP treatment, animals were anesthetized in an enclosed chamber and were then perfused transcardially with 4% (w/v) paraformaldehyde (PFA) that served as a fixative. The mouse brains were then carefully removed and post-fixed in 4% (w/v) PFA for 12 h at 4°C, followed by transfer to 30% (w/v) sucrose in phosphate buffered saline (PBS) at 4°C for ~36–48 h. The brains were then embedded in tissue freezing medium (Leica

Microsystems Nussloch GmbH Cat. No. 0201 08926). Serial coronal sections (25 µm thickness) were cut through the midbrain region of the brain.

TH immunohistochemistry: Serial coronal sections preserved in Tris buffered saline (TBS) with sodium azide (0.005% w/v) were used for IHC. Sections were washed twice with TBS (5 min) and incubated with blocking solution (3% (w/v) bovine serum albumin (BSA), 0.1% (v/v) Triton-X 100, and 3% (v/v) normal horse serum in TBS) for 1 hour at room temperature followed by incubation in rabbit anti-TH (Millipore Cat. No. AB152, RRID: AB\_390204) (1:500) in TBS-Tween 20 (TBST) for 12 h at 4°C. Further, sections were given four washes with TBST and incubated in donkey anti-rabbit IgG H+L (Alexa Fluor 594) (Thermo Scientific A-21207, RRID: AB\_2556547) (1:1000) in TBST for 1 hour. The sections were then washed and mounted in VECTASHIELD mounting medium with DAPI (Vector Laboratories Cat. No. H-1200) on glass slides.

Stereological analysis on histological data: Analysis of total number of TH positive neurons in SNpc was performed for every sixth coronal section through the midbrain using Stereo Investigator by MBF Bioscience (RRID:SCR\_002526). All data were quantified in an experimentally blind manner.

The sections were imaged on an Olympus microscope using the Stereo Investigator (MBF Bioscience) software to obtain tile scans of unilateral SNpc across z (vertical axis) at a magnification of 40×. Counting was performed in an experimentally blind manner, offline using the optical fractionator probe (Gundersen and Jensen 1987; West et al. 1991) using 60 × 60 µm counting frame at x = 150 µm, y = 150 µm intervals from a random start point. A guard zone of 2.5 µm, and a probe depth of 20 µm were used. The coefficient of error was below 0.1 in all animals studied.

Mouse brain SNpc dissection: MPTP treated mice were decapitated following cervical dislocation post 24 h of the last dose of MPTP in the treatment paradigm following cervical dislocation. Mouse brain was placed on mouse brain matrix (Ted Pella, Inc Cat. No. 15050) and 1 mm thick slices of the brain were obtained for the dissection of SNpc, under cold and sterile conditions. Then, SNpc was dissected out from these slices under stereomicroscope using anatomical markers.

Human brain tissue dissection: For the dissection of SNpc, slides containing cryostat-cut sections of flash frozen human autopsy midbrain tissue from PD patients and age-matched controls were obtained from the ICM Brain Bank and the Neuroceeb Pitié-Salpêtrière hospital, Paris. Controls were individuals without neurologic or psychiatric disorders. Patients with PD displayed the characteristics of the disease including akinesia, rigidity and/or resting tremor. All patients with PD were treated with dopaminergic agonists and/or L-DOPA and displayed or had displayed dyskinesia. The clinical diagnosis was confirmed by neuropathological examination including the presence of Lewy bodies at least in the substantia nigra. Mean post-mortem delay and age at death did not differ between controls and patients with PD. A table with details on patients has been appended in **Table. 1** and supplementary (supplementary table S1). SNpc was scraped off the surface of the slides, kept on dry ice under sterile conditions using anatomical landmarks.

RNA isolation: All the reagents used for RNA isolation and cDNA synthesis were prepared in RNAase free conditions using DEPC water. RNA from mouse brain tissue was isolated using TRIzol reagent (Invitrogen Cat. No. 15596018) and bromochlorophenol (BCP) (Molecular Research Centre, Inc. Cat. No. BP151) (Chomczynski

and Sacchi 2006). RNA was isolated from human autopsy brain tissue using the RNeasy Plus Universal Mini Kit (Qiagen Cat. No. 73404).

RNA quality check, cDNA library preparation and RNA sequencing: Integrity and purity of RNA samples was determined using Nanodrop, Qubit and BioAnalyzer and samples with Rin value less than 5 were not used. The NEBNext Ultra Directional RNA Library Prep Kit for Illumina (NEB Cat. No. E7420G, 30061409) was used for preparing the strand specific libraries from mouse RNA. The sequencing was performed in paired end manner, generating  $2 \times 75$  bp long reads and a total of 44-50 million reads. RNA-seq library preparation for human tissue samples was performed using the TruSeq RNA Library Prep Kit v2 (Catalog IDs: RS-122-2001, RS-122-2002). These libraries were prepared in an unstranded manner. The sequencing was performed in paired end manner, generating  $2 \times 100$  bp long reads and a total of about 40 million reads. While RNA sequencing on mouse SNpc libraries was performed on Illumina HiSeq2000, RNA-seq on human SNpc libraries was performed on Illumina HiSeq2500.

Differential gene expression and pathway analysis: Analysis of RNA-seq data was performed on Linux operating system Debian GNU/Linux 8 (Jessie). The raw sequencing data, in the form of FastQ files was checked for quality using FastQC (RRID:SCR\_014583), following which the low quality reads and adapter sequences were removed using Trimmomatic (v0.36; RRID:SCR\_011848) (Bolger et al. 2014). Further, TopHat2 (v2.1.1; RRID:SCR\_013035) (Kim et al. 2013) was used for alignment of reads to mouse or human genomes. Ensembl genome GRCm38 was used as mouse genome reference genome and GRCh37 was used as human reference genome. The resultant alignment files are in the bam (binary alignment/map) format, which were

further sorted in the order of names of genes using Samtools (v0.1.19; RRID:SCR\_002105) (Li et al. 2009) and finally the numbers of counts for each read in each sample were generated using htseq-count (Anders et al. 2015). DESeq2 version 1.22.2 (Love et al. 2014)( RRID:SCR\_015687) was used for normalization of read counts. DESeq2 analysis was performed on R version 3.5.1 (RRID:SCR\_001905).

Normalization by Cufflinks methods (Trapnell et al. 2012) was repeated on the human data after alignment by following the Cufflinks (v2.2.1; RRID:SCR\_014597): Cuffmerge-Cuffdiff pipeline and differentially expressed genes were identified for validation of DESeq2 data.

Data on differential gene expression of developmental genes was also validated by the changing the DESeq2 linear model to account for age, post-mortem interval (PMI) and RIN. The altered model was: ~age+PMI+RIN+condition. All subsequent data analysis was performed on genes that were differentially expressed and had adjusted p values less than 0.05 as determined using DESeq2 normalization.

Functional annotation clusters from differentially expressed genes that were significantly different were created using the Database for Annotation, Visualization and Integrated Discovery (DAVID) bioinformatics resources 6.8 (RRID:SCR\_001881) (Huang et al. 2009b, a) and GOpot 1.0.2 (Walter et al. 2015) was used for visualization of the data. The pheatmap 1.0.12 (RRID:SCR\_016418) (Kolde 2012) was used for generation of heatmaps and volcano plots were created using EnhancedVolcano 1.5.0 (RRID:SCR\_018931) (Blighe et al. 2019). Protein-protein associations that may result from co-differential expression of genes were drawn using String database

(RRID:SCR\_005223) (Szkłarczyk et al. 2019). The Venn diagrams were plotted using the tool available at the url: <http://bioinformatics.psb.ugent.be/webtools/Venn/>.

**Representation of cell-type specific markers:** The analysis of the presence of markers of different cell-types in substantia nigra was performed by using the data base curated by Mancarci et al.(Mancarci et al. 2017) The overlap between the cell-type specific markers in different SN cell-types and the significantly differentially expressed genes was determined.

**Cell-type specific analysis of differential gene expression:** Reference-based differential expression of genes specifically in dopaminergic neurons from human SN was estimated using the package TOAST (Li and Wu 2019; Li et al. 2019) in R. The reference matrix for estimation of proportional expression of genes in different cell types in the substantia nigra was generated from the single cell RNA sequencing data (GSE140231) published by Agarwal and colleagues (Agarwal et al. 2020) analyzed using the package Seurat (RRID:SCR\_016341) (Hao et al. 2021) in R.

**Projected network analysis on human differentially expressed genes:** Gene expression data generated by performing microarray on human post-mortem brain tissue from neurologically and neuropathologically control individuals was used for the construction of basal gene expression network using weighted gene co-expression network analysis (WGCNA; RRID:SCR\_003302). Normalised gene expression data (GSE46706) was obtained from GEO database. WGCNA (version1.51) on the SN dataset resulted in generation of 16 co-expression modules. The significantly differentially expressed genes from DESeq2 analysis were matched to each of the modules using hypergeometric test (performed on R) to calculate the significant representation of the DESeq2 genes within

each of the modules. This data was then used to create network using Cytoscape version 3.5.1 (RRID:SCR\_003032).

Quantitative real time PCR: Human total RNA (200 ng) was used for first strand cDNA synthesis using random hexamers, dNTPs and reverse transcriptase from the high capacity cDNA reverse transcription kit (Applied Biosystems Cat. No. 4368814). Quantitative real time PCR (qRT-PCR) was performed using SYBR green chemistry for *GAP43*, *RET*, *LMX1B*, *EN1* and *DAT*. The nucleotide sequences for primers used for human tissue gene expression analysis are provided in supplementary table S2. Two endogenous controls, namely β-actin and *GAPDH* were used for normalization. For mouse SNpc samples, qRT-PCR was performed using SYBR green chemistry for *Dat*, *Th*, *Lmx1b*, *En1*, *Ret* and *Gap43*. The nucleotide sequences for primers used for mouse tissue gene expression analysis are provided in supplementary table S3. The qRT-PCR conditions are provided in supplementary table S4. 18S rRNA was used for normalization.

*LMX1B-GFP* over expression construct: Expression construct for human *LMX1B* was subcloned from the tetO-ALN plasmid (Addis et al. 2011). tetO-ALN was a gift from John Gearhart (Addgene plasmid No. 43918; <http://n2t.net/addgene:43918>; RRID: Addgene\_43918). The open reading frame (ORF) for human *LMX1B* was PCR-amplified using the following primer sequences: Forward primer: 5'-HindIII-GACGTCAAGCTTGCACCATGTTGGACGGCATCAAG-3'; Reverse primer: 5'-BamHI-GACCGGTGGATCCGCGGAGGCGAAGTAGGAAC-3'. The ORF thus PCR-amplified was sub-cloned at the multiple cloning site of pEGFP-N1 between HindIII and BamHI

restriction enzyme sites following standard ligation and bacterial transformation protocol.

Experiments with SH-SY5Y cells: SH-SY5Y cells (ATCC CRL-2266; RRID:CVCL\_0019) were cultured in Minimum Essential Medium Eagle (MEM; Sigma, Cat. No. M0643) that was supplemented with 10% v/v fetal bovine serum (FBS; Gibco, Cat. No. 26140079, Origin: U.S) and 1X penicillin-streptomycin (Gibco, Cat. No. 15070063). SH-SY5Y cells were plated at a confluence of 70% on glass cover slips (VWR, Cat. No. 26022) that were acid washed and precoated with poly-D-lysine (0.1 mg/ml) in 12-well plates.

Within ~16 hours of plating, SH-SY5Y cells were transfected with *LMX1B* in pEGFP-N1 or pEGFP-N1 (control plasmid) using Lipofectamine LTX Reagent with PLUS Reagent (Invitrogen, Cat. No. 15338030) in OptiMEM medium (Gibco, Cat. No. 22600-050). The media was changed to MEM with FBS and penicillin-streptavidin after 6 hours.

SH-SY5Y cells were treated with MPP<sup>+</sup> (1mM; Sigma-Aldrich D048) 48 hours after transfection with *LMX1B* in pEGFP-N1 or pEGFP-N1 (control plasmid). The cells were washed with PBS and fixed with 2% paraformaldehyde (w/v) 24 hours after MPP<sup>+</sup> exposure. For immunoblotting of *LMX1B-GFP* overexpression,, 48 hours post transfection, SHSY5Y cells were washed with ice cold PBS (pH7.4) and lysed in an ice cold RIPA buffer containing 50 mM Tris-HCl, (pH 7.4), 150 mM NaCl, 1 mM EDTA, 1% Nonidet P-40, 0.5% Sodium Deoxycholate, 0.1% SDS and supplemented with phosphatase (50 mM sodium fluoride, 1 mM sodium orthovanadate) and protease inhibitors (2 µg/ml aprotinin, 10 µg/ml leupeptin, 7 µg/ml pepstatin A, 100 µg/ml of phenylmethanesulfonyl fluoride (PMSF), benzamidine (100 µM), and 50 µg/ml anti-

pain. The cell lysate was centrifuged at 16000 x g for 30 min at 4°C. After centrifugation, protein concentrations were measured by bicinchoninic acid (BCA) protein assay, and equivalent protein was used for immunoblotting.

The extent of cell death following MPP<sup>+</sup> treatment with pEGFP-N1 and *LMX1B-GFP* overexpression was assessed by using the terminal deoxynucleotidyl transferase mediated dUTP-biotin nick end-labeling (TUNEL) method (In situ cell death detection kit, TMR red, Roche, Cat. No. 12156792910), according to the manufacturer's protocol. Ten fields were imaged from three independent coverslips for each experimental condition. Analysis was performed to quantify the average number of TUNEL-positive (Red) cells and was blinded.

Statistics: Samples were analyzed in triplicates. Relative gene expression was analyzed using  $\Delta\Delta Ct$  method. Data was analyzed and represented using Graphpad Prism (Graphpad Prism Inc, USA; RRID:SCR\_002798). Statistical significance was determined using Student's *t* test. All data are presented as mean  $\pm$  SEM.

## Results

### Gene expression changes in mouse model of PD using MPTP

RNA sequencing was performed on SNpc, dissected (Fig. 1A) from mice treated with a single dose (acute) of MPTP (30 mg/kg body weight) or daily for 14 days (chronic). While single dose of MPTP represents the first hit without substantial cell loss; about 30% loss of dopaminergic neurons is seen after 14 days of MPTP treatment (Saeed et al. 2009). Indeed, stereological examination of tyrosine hydroxylase (*Th*) positive neurons in SNpc revealed a 27% reduction in total number of dopaminergic neurons (Fig. 1B). Further, down-regulation of several dopaminergic genes such as, dopamine transporter (*Dat*), DOPA decarboxylase (*Ddc*) and vesicular monoamine transporter 2 (*Vmat2*) was observed after 14 days of MPTP treatment (Fig. 1C) but not after single exposure. Only *Th* was downregulated after both one and 14 days of MPTP treatment.

Differential gene expression analysis of RNA-seq data from mouse SNpc (n = 5 controls and 5 treated mice) after 24 hours following single exposure to MPTP revealed significantly (adjusted p <0.05) altered expression of 472 genes, 291 of which were upregulated and 181 were down-regulated (Fig. 1D and 1F). However, analysis of data from mouse SNpc (n = 3 controls and 3 treated mice) after 14 days of MPTP treatment showed significant (adjusted p <0.05) altered expression of 74 genes, 23 of which were upregulated and 51 were downregulated (Fig. 1E and 1G). Thus, fewer genes were perturbed as the disease progressed and cell loss continued. As evident from the Venn diagram (Fig. 1H), there was little overlap between the two sets suggesting the involvement of different molecular pathways during early and later stages of MPTP

treatment. Further, there was greater perturbation in terms of number of differentially expressed genes 24 hours after single dose of MPTP, which could be due to the adaptive response to the toxin. Analysis of cell-type specific markers expressed among the differentially expressed genes 24 hours after a single dose of MPTP revealed differential expression of markers of oligodendrocytes, microglia, astroglia, and dopaminergic neurons (supplementary Fig. S1A). However, a similar analysis for the differentially expressed genes after 14 days of MPTP treatment revealed differential expression of dopaminergic neuron markers and only one marker of microglia (supplementary Fig. S1B). A complete list of the differentially expressed genes is provided in the supplementary tables S5 and S6. (*Figure. 1 should be placed here*)

Perturbation of different pathways seen at early and late stage of MPTP mouse model of PD

Identification of gene ontology (GO) pathways including biological processes (BP), molecular function (MF), and cellular components (CC), which were populated by genes that were significantly up or downregulated in SNpc after single exposure to MPTP revealed an upregulation of pathways, such as innate immune response, inflammatory response, response to cytokine, cellular response to tumor necrosis factor, apoptotic processes, and MAPK cascade, and a downregulation of pathways, such as nervous system development (Fig. 2A and supplementary table S7). A similar analysis for the RNA-seq data from 14 days MPTP mouse SNpc did not show perturbation of innate immune response or inflammatory response. However, upregulation of pathways involved in functioning of extracellular exosome and downregulation of pathways

involved in functioning of, response to nicotine, regulation of dopamine metabolic process, and synapse (Fig. 2B and supplementary table S8).

The circular plots for acute (Fig. 2C) and chronic (Fig. 2D) MPTP treatment shows hierarchical clustering of the significant genes based on functional categories and how they populate these categories along with their  $\log_2$  fold change. Further, chord diagrams for differentially expressed pathways and their resident genes after single dose (Fig. 2E) and 14 days (Fig. 2F) of MPTP treatment show the significantly differentially expressed genes that populate at least three different pathways and their  $\log_2$  fold change. (*Figure. 2 should be placed here*)

The early stage of MPTP mouse model thus presents a canvas of molecular pathways that is quite dissimilar to what is observed at late stage of the model. It is also intriguing to note the absence of differentially expressed genes related to innate immunity and inflammatory response in SNpc from mouse treated with MPTP for 14 days, wherein about 30% of dopaminergic neurons are lost.

#### Gene expression changes in SNpc from human PD

The anatomical landmarks used for dissection of SNpc are depicted in Fig. 3A. The top 30 differentially expressed genes are tabulated in Fig. 3B. Differential gene expression analysis through DESeq2 revealed significantly (adjusted p <0.05) altered expression of 367 genes, of which 103 were upregulated and 264 were downregulated in SNpc of human PD brain (n= 3 controls and 4 PD patients; Fig. 3C and 3D).

Complete list of differentially expressed genes is provided in supplementary table S9. Markers of dopaminergic neuron phenotype such as *DAT*, *VMAT2*, *DDC*, *DRD2* and *TH* were significantly downregulated (Fig. 3E), which served as a positive indication of degeneration of dopaminergic neurons in SNpc in these samples. Components of the ubiquitin-proteasome pathway such as, *PSMD12*, *UBE2T*, *UBFD1* and *UCHL1* were downregulated in the human PD. Of the genes that were downregulated, *UCHL1* (also known as *PARK5*) has been associated with familial PD (Maraganore et al. 2004). Dysregulation of the ubiquitin-proteasome pathway is one of the well-studied mechanisms implicated in the pathogenesis of PD (Cook and Petrucelli 2009). Further, analysis of cell-type specific markers expressed among the differentially expressed genes revealed differential expression of markers of dopaminergic neurons, microglia (deactivation, genes are downregulated in activated microglia), and astroglia (supplementary Fig. S1C). (*Figure. 3 should be placed here*)

Neuron specific genes such as *MAP2*, *RBFOX3* and *TUBB3* were unchanged in human PD. Further, the mRNA expression of β-actin and glyceraldehyde 3-phosphate dehydrogenase (*GAPDH*), as assessed using qRT-PCR, remained unchanged as seen after normalization with ribosomal protein L13 (*RPL13*) in human PD (supplementary Fig S3).

Pathway analysis reveals down regulation of dopaminergic neuron differentiation factors in human PD

Pathway analysis, performed using the significantly differentially expressed genes, showed downregulation of functional clusters, such as those involved in synaptic vesicle recycling, regulation of synaptic plasticity, dopaminergic neuron differentiation

and locomotory behavior (Fig. 4A and supplementary table S10). We also clustered significantly expressed genes according to functional categories (Fig. 4B). Further, the chord diagram shows distribution of differentially expressed genes in pathways with their adjusted p values (Fig. 4C). An interesting set of genes that were perturbed significantly as highlighted is of those that belong to dopaminergic neuron differentiation as also those that define midbrain dopaminergic neuron development and maintenance. These include *FOXA1*, *RSPO2*, *KLHL1*, *LMX1B*, *EBF3*, *PITX3*, *RGS4*, *ALDH1A1*, *RET*, *FOXA2*, *EN1*, *DLK1*, *GFRA1*, *LMX1A*, *NR4A2*, *GAP43*, *SNCA*, *PBX1* and *GRB10* (Fig. 4D). (*Figure. 4 should be placed here*)

Weighted gene co-expression network analysis (WGCNA) on the SN dataset obtained from GEO database resulted in generation of 16 modules as described in the Methods section. Significantly differentially expressed genes from DESeq2 analysis were matched to each of the modules using hypergeometric test to calculate the significant representation of the DESeq2 genes within each of the modules. Only one out of 16 modules showed significant representation of the DESeq2 genes. All the correlations of the DESeq2 genes within this module were then isolated with the weights of correlation. This dataset now has information on a gene, every other gene that it co-expressed with and the weight of correlation. This data was used to create network using Cytoscape v3.5.1. The resultant network was highly dense (supplementary Fig. S2).

All the genes in the network that are downregulated were classified into genes that are markers of dopaminergic neurons, gene involved in synaptic vesicle release, ubiquitin proteasomal system and genes important for development and maintenance of

dopaminergic phenotype. Several genes that are important markers of dopaminergic phenotype were represented in the network. These genes included *TH*, *DOPA*, *DDC*, *DAT*, *DRD2*, and *VMAT2*. Several genes that are important for development and differentiation of dopaminergic neurons were also observed in the network. These genes involved include *LMX1B*, *FOXA1*, *EN1*, *DLK1*, *RET*, *KLHL1*, *EBF3*, *GDNF*, *GFRA1*, and *GAP43*.

Further, we validated the downregulation of the genes belonging to the pathway related to differentiation of midbrain dopaminergic neurons, namely, *GAP43*, *RET*, *LMX1B* and *EN1* in SNpc from PD autopsy tissue using qRT-PCR. Evaluation of *TH* mRNA was not performed since four different isoforms exist in the human brain (Grima et al. 1987; Lewis et al. 1993) while a single *TH* isoform is present in the mouse brain (Iwata et al. 1992), creating difficulty in choosing a single *TH* sequence as a suitable reference marker for qRT-PCR in human tissue. Down-regulation of *DAT*, a marker for dopaminergic neurons was seen (Fig. 5A), which is expected following dopaminergic neuronal death in SNpc. This is indeed an interesting observation considering that genes involved in differentiation of dopaminergic phenotype are indeed important for its maintenance and their downregulation could impact the health of dopaminergic neuron.

We further validated the downregulation of genes using an alternate method of normalization, that is, Cufflinks and also after regressing the data for age, post mortem interval (PMI) and RIN using DESeq2 (supplementary tables S11 and S12) and found that majority of the selected genes were significantly downregulated through both the analyses. Moreover, we performed cell-type specific analysis after estimation of cell type proportions on dopaminergic neurons from the data from PD patients to account for

the presence of other cell types, namely, astrocytes, microglia, and oligodendrocyte precursor cells and showed that many of the selected genes were downregulated in the dopaminergic neurons specifically (supplementary table S13). Though the downregulation of *GAP43* does not have a significant adjusted p value but only a significant p value, it was significantly downregulated in the qRT-PCR experiments.

The RNA-seq data from mouse SNpc following MPTP treatment for 14 days did not show significant adjusted p values for *Lmx1b*, *En1* and *Ret* even though the raw reads had decreased by 39, 18 and 37%, respectively. However, these genes were significantly downregulated when examined using qRT-PCR (Fig. 5B). The downregulation of these genes in mouse model of PD demonstrate that the dysregulation of this pathway occurs both in mouse and human. (*Figure. 5 should be placed here*)

Protein-protein interactions that can potentially result from co-expression changes in the genes involved dopaminergic neurons differentiation, is depicted in Fig. 6A using String database (Szklarczyk et al. 2019). Further, mapping these interactions based on existing data (Fig. 6B) revealed *LMX1B* as an important gene upstream to the expression of many genes involved in dopaminergic midbrain neuron development, differentiation and maintenance. Thus, we see that the whole ensemble of genes (*LMX1B*, *FOXA1*, *RSPO2*, *KLHL1*, *LMX1B*, *EBF3*, *PITX3*, *RGS4*, *ALDH1A1*, *RET*, *FOXA2*, *EN1*, *DLK1*, *GFRA1*, *LMX1A*, *NR4A2*, *GAP43*, *SNCA*, *PBX1* and *GRB10*) that are essential for dopaminergic neuron development, differentiation and maintenance are downregulated in human PD, including those that are downstream of *LMX1B*.

Therefore, we overexpressed *LMX1B* and assessed its effect on MPP<sup>+</sup> mediated cell death.

***LMX1B* overexpression rescues SHSY-5Y from MPP<sup>+</sup> toxicity**

Recombinant human *LMX1B*-GFP was over expressed in SH-SY5Y neuronal cell line, as confirmed by immunoblotting (Fig. 6C; supplementary Fig. S4), which were then exposed to parkinsonism-inducing toxin, MPP<sup>+</sup>. We observed that while exposure to MPP<sup>+</sup> led to significant death in SH-SY5Y cells as measured using TUNEL assay, overexpression of *LMX1B*-GFP led to significant reduction in the percentage of TUNEL positive cells (Fig. 6D and 6E). Our results, therefore, show that *LMX1B* is capable of rescuing SH-SY5Y cells from MPP<sup>+</sup> mediated cell death. (*Figure. 6 should be placed here*)

## Discussion

In this study, global changes in the transcriptome were studied in precisely dissected substantia nigra pars compacta (SNpc) from MPTP mouse model of PD after acute and chronic MPTP treatment using RNA sequencing (supplementary Fig. S5). Further, RNA sequencing was also performed on SNpc from PD patients and age-matched controls. A single dose of MPTP resulted in a larger number of differentially expressed genes in mouse SNpc as compared to 14 days treatment with MPTP. Gene expression changes in SNpc from mice after single exposure to MPTP resulted in dysregulation of pathways related to immune and inflammatory system. However, after 14 daily doses of MPTP and in human PD, these pathways were not enriched. While Riley and colleagues have indeed reported dysregulation of several inflammatory pathways (Riley et al. 2014), it is essential to note that the RNA-seq in their study was performed on substantia nigra which would include contribution from the GABA-ergic neurons of pars reticulata. The present study, on the other hand, evaluates gene expression changes in specifically substantia nigra pars compacta, which could explain the observed difference. Further, a recent transcriptomic study describes gene expression alteration in SN from the brain of PD patients in relation to Braak staging (Keo et al. 2020). Using co-expression analysis, Keo and colleagues have reported the dysregulation of genes related to dopamine synthesis, microglia, immune system, blood-oxygen transport, and endothelial cells. However, in the present study, when we analyzed only the significantly differentially expressed genes, we were able to identify the downregulation of an ensemble of genes involved in development and differentiation of midbrain dopaminergic neurons as a novel pathway involved in PD pathogenesis.

We, further, confirmed downregulation of these genes using qRT-PCR and validated the protective effect of overexpression of an upstream regulator of this pathway, namely, *LMX1B*, against MPP<sup>+</sup> induced cell death in SHSY-5Y cells.

When we compared the transcriptomic changes observed in 14 days MPTP mouse SNpc with human PD, we found similarity in terms of downregulation of the common genes involved in dopaminergic phenotype maintenance. Further, several pathways that were dysregulated in the 14 days MPTP mouse SNpc were similar to those observed to be perturbed in a microarray study on induced pluripotent stem cells-derived dopaminergic neurons from PD patients (Fernández-Santiago et al. 2015).

While few dysregulated pathways are common between MPTP model and human PD, the differences are predominant reinforcing the limited overlap of the molecular pathways involved in neurodegeneration. However, it is also to be noted that while the MPTP mouse model mimics substantia nigra degeneration, these mice do not recapitulate other lesions and consequently do not show all the symptoms of PD. Moreover, the differences observed could have stemmed from various other factors, such as species differences, the disease pathology being chronic, over days in humans as opposed to acute for only a few days/weeks for the mouse model, the status of the disease being end stage PD in humans versus early phase in animals, and the contribution of the loss of other neurons that might in turn affect dopaminergic neurons whereas in the model there is only a loss of dopaminergic neurons. These factors could explain the small number of common molecular pathways that were dysregulated in the mouse model and in PD brain.

The low log<sub>2</sub> fold change values observed for some of the statistically significantly differentially expressed genes could potentially be attributed to the limitations of bulk RNA sequencing. In addition to the neurons, the dissected SNpc tissue will also have contribution from other glial cell types. Moreover, while ~70% of rodent SNpc neurons are dopaminergic, about 29% are GABAergic and 1–2% are glutamatergic (Nair-Roberts et al. 2008). Thus, the actual fold change in gene expression that may stem specifically from SNpc dopaminergic neurons may get diluted due to the presence of other cell types. We are aware of this limitation; however, it is still important to study gene expression in the surviving dopaminergic neurons.

Two striking observations of this study are the lack of enrichment of genes involved in inflammatory and immune response and the downregulation of an entire ensemble of genes in SNpc from patients with PD that are well characterized for their role in maintenance of dopaminergic phenotype, namely, *FOXA1*, *RSPO2*, *KLHL1*, *LMX1B*, *EBF3*, *PITX3*, *RGS4*, *ALDH1A1*, *RET*, *FOXA2*, *EN1*, *DLK1*, *GFRA1*, *LMX1A*, *NURR1*, *SNCA*, *PBX1*, and *GRB10* in human PD (Thuret et al. 2004; Jacobs et al. 2009; Lei et al. 2011; Alavian et al. 2014; Domanskyi et al. 2014; Kramer and Liss 2015; Blaudin de Thé et al. 2016; Drinkut et al. 2016). The downregulation of these genes could presumably affect the expression of genes that define the dopaminergic phenotype, such as *DAT*, *TH*, *DRD2* and *DDC*. *GAP43* has been implicated in neurogenesis and its role in survival or maintenance of dopaminergic neurons is not clear (Murakami et al. 2007, 2011). A customized pathway analysis to investigate the enrichment of the differentially expressed genes also revealed the enrichment of the module containing genes important for dopaminergic phenotype. Further, a recent

single cell transcriptomic study (Agarwal et al. 2020) performed using human substantia nigra also demonstrated the expression of the genes including *RSPO2*, *KLHL1*, *LMX1B*, *EBF3*, *RGS4*, *ALDH1A1*, *RET*, *EN1*, *GFRA1*, *NURR1*, *SNCA*, and *PBX1* in the dopaminergic neurons in SN suggesting the importance of these genes in SN.

A summary of the functions of genes involved in development, differentiation and maintenance of dopaminergic neurons is presented in Fig. 6B. Sonic hedgehog (*SHH*), *WNT1* and *FGF8* are important early genes that induce the expression of *FOXA2*, *LMX1A*, *LMX1B* and *EN1* during the earliest stages of midbrain dopaminergic neuron development, which further drive the expression of *NURR1* and *PITX3* and thereby lead to expression of *TH*, *VMAT2*, *DRD2*, *DDC*, *DAT* and *ALDH1A1* that define the dopaminergic neuron phenotype (Simon et al. 2003; Prakash and Wurst 2006; Abeliovich and Hammond 2007; Hegarty et al. 2013; Arenas et al. 2015; Bissonette and Roesch 2016; Smidt 2017). Further, studies have implicated the role of genes such as *RGS4*, *GRB10* and *RSPO2* that are downstream *LMX1A* in midbrain dopaminergic neurogenesis and differentiation (Hoekstra et al. 2013b, a). Similarly, there is evidence that *EBF3* may lie upstream of *NURR1* and *PITX3* (Baek et al. 2014) and *PBX1* is upstream of *PITX3* and *EN1* (Veenvliet et al. 2013; Villaescusa et al. 2016; Kouwenhoven et al. 2017) and may play an important role in dopaminergic neuron development. Moreover, the expression of *NURR1* and *PITX3* is induced by *GDNF/RET* signaling and has been shown to be important for protection of dopaminergic neuron (Peng et al. 2011; Kramer and Liss 2015). It is also important to note that several studies have emphasized on the strong co-ordination among the members of this pathway such as *NURR1* and *FOXA2*, *PITX3* and *EN1*, *NURR1* and *EN1* and *FOXA2*.

and *LMX1A* and *B* (Lin et al. 2009; Lee et al. 2010; Veenvliet et al. 2013; Alavian et al. 2014; Kouwenhoven et al. 2017).

While these genes are indispensable for the development of midbrain dopaminergic neurons, fewer studies have assessed their function in the adult SNpc. *EN* genes have been reported to be essential for survival of midbrain dopaminergic neurons and regulate the expression of  $\alpha$ -synuclein (*SNCA*) (Simon et al. 2001). *LMX1A/B* have been shown to be important for maintenance of dopaminergic neuron phenotype through their roles in regulating normal autophagic-lysosomal pathway (Laguna et al. 2015) and mitochondrial functions (Doucet-Beaupré et al. 2016).

In the present study, we have observed the concomitant down-regulation of majority of the genes important for development and maintenance of dopaminergic neurons, which not only emphasize the role that this pathway plays in the pathogenesis of PD but also the interdependence of these genes in dopaminergic neuron survival. However, how these genes are downregulated so specifically in SNpc from patients with PD and their roles in the adult SNpc needs to be addressed. Importantly, we demonstrated that the overexpression of *LMX1B-GFP*, which is an upstream regulator of the midbrain dopaminergic neuron differentiation pathway, can rescue cell death as a result of MPP<sup>+</sup> toxicity in the SH-SY5Y neuron cultures suggesting that a revival of this pathway could potentially rescue neurodegeneration in PD.

It is to be noted that while we have carried out cell type specific analysis on the data, there is a differential cell composition in the substantia nigra pars compacta which is contributed to the controls by just aging and in the PD brains by aging and disease. This is inherent problem in using autopsy tissues, which is well recognized but

nevertheless the identification of *LMX1B* as a major upstream regulator, which is dysfunctionally regulated in PD is very significant.

While greater emphasis has been given to addressing the motor dysfunctions observed in PD, management of non-motor symptoms of PD including sleep and autonomic dysfunction, and psychiatric symptoms is increasingly becoming a larger burden. While two loci associated with *SNCA* have been identified as risk loci in a PD genome wide association study (GWAS)(Nalls et al. 2019), interestingly, a review of GWAS revealed the association of *ALDH1A1* (Greenwood et al. 2019) and *DRD2* (Consortium 2014) with schizophrenia. *DRD2* is also associated with alcohol consumption (Evangelou et al. 2019) and sleep deprivation (Lane et al. 2017). *NURR1* (Zhou et al. 2017) and *LMX1A* (Brazel et al. 2019) are associated with alcohol consumption while *DAT* (Jansen et al. 2019) and *PBX1* (Spada et al. 2016) are associated with sleep duration. Further *RET* has been associated with cannabis dependence (Sherva et al. 2016) and smoking behavior (Matoba et al. 2019). Thus, we see that several of the genes dysregulated in PD are associated with addictive behavior and impact a variety of behavioral dysfunctions which co-occur with PD. The impact of downregulation of the genes as we see in the present study would potentially have far-reaching effects beyond motor symptoms. However, the present study being exploratory in nature, further studies with larger sample size are warranted to confirm and better understand the role of these genes in PD.

In conclusion, we demonstrate for the first time that an ensemble of 19 genes that govern and regulate the development of midbrain and emergence of dopaminergic phenotype in SNpc neurons are markedly downregulated in the PD samples analyzed in

our study. These not only include genes that are downstream of LIM homeobox transcription factor, *LMX1B* (*PITX3* and *ALDH1A1*) and *LMX1A* (*GRB10*, *RGS4*, *RSPO2*, *NURR1*, *KLHL1*, *DLK1* and *RET*), but also other genes that are upstream such as, *FOXA2* and *RET* and genes regulated by *FGF8* such as *EN1*; indicating that these genes are potentially important for the maintenance of dopaminergic neurons.

Interventions that could potentially upregulate the key genes that lie upstream in this cascade could protect dopaminergic neurons and thus alter the progression of the disease. Thus, identification of this ensemble offers a new window for discovery of disease modifying therapies for PD.

## Acknowledgements

The authors declare no other financial disclosures. The authors are grateful to Dr Charles Duyckaerts for the neuropathological examination Annick Prigent from the ICM Histomics platform and Sabrina Leclerc-Turbant from Neuroceb for their help in preparing the human post-mortem samples. We thank Priya Suresh and Rehab Hussain for helping with TUNEL experiments. We also thank Prof. David A Bennett and Dr. Chris Gaiteri at the Rush University Medical Centre, Chicago, USA for helpful discussions.

## Declarations

### Author Contributions

Research project was conceptualized by VR, organized by AV, EH and VR and executed by AV, RPK and BG. Statistical analysis was designed and executed by AV, RPK, and reviewed and critiqued upon by EH and VR. First draft of the manuscript was written by AV and VR and was further reviewed and critiqued upon by EH. All authors read and approved the final manuscript.

### Author Affiliations

Aditi Verma: Centre for Neuroscience, Indian Institute of Science, Bangalore-560012, India

Reddy Peera Kommaddi: Centre for Brain Research, Indian Institute of Science, Bangalore-560012, India

Barathan Gnanabharathi: Centre for Brain Research, Indian Institute of Science, Bangalore-560012, India

Etienne C. Hirsch: Sorbonne Université, Institut du Cerveau – ICM, Inserm U 1127,  
CNRS UMR 7225, F-75013, Paris, France

Vijayalakshmi Ravindranath: Centre for Brain Research, Indian Institute of Science,  
Bangalore-560012, India

#### ORCIDs

Aditi Verma: 0000-0002-6771-576X

Reddy Peera Kommaddi: 0000-0002-5874-944X

Barathan Gnanabharathi: 0000-0001-9996-0578

Etienne C. Hirsch: 0000-0003-4823-276X

Vijayalakshmi Ravindranath: 0000-0003-3226-0782

#### Competing Interests

The authors declare that there are no competing interests.

#### Funding

The study was funded by TATA Trusts and Scientific Knowledge for Ageing and Neurological ailments (SKAN) Research Trust (VR). AV received research fellowship from Council of Scientific and Industrial Research (CSIR), Government of India. EH acknowledges the financial support from CNRS, INSERM, ICM, UPMC and from the program “Investissements d’avenir” ANR-10-IAIHU-06.

#### Ethics Approval

Animal experiments were approved by the institutional animal ethical review board, named ‘Institutional Animal and Ethics Committee’ of Indian Institute of Science (Protocol No. CAF/Ethics/267/2012). Animals were handled according to the guidelines

of Committee for the Purpose of Control and Supervision of Experiments on Animals (CPCSEA), Government of India.

All experiments on human autopsy brain tissue were carried out following approval from Institutional Human Ethics Committee of the Indian Institute of Science and all guidelines were followed (IHEC approval No. 10/1/2015).

#### Data Availability Statement

The data that support the findings of this study are provided within the paper and its supplementary information. Raw RNA sequencing data have been deposited into the National Center for Biotechnology Information Gene Expression Omnibus under accession number GSE206308.

#### Consent to participate

Informed consent was obtained from subjects included in the study.

## References

- Abeliovich A, Hammond R (2007) Midbrain dopamine neuron differentiation: Factors and fates. *Dev Biol* 304:447–454. <https://doi.org/10.1016/j.ydbio.2007.01.032>
- Addis RC, Hsu F-C, Wright RL, et al (2011) Efficient conversion of astrocytes to functional midbrain dopaminergic neurons using a single polycistronic vector. *PLoS One* 6:e28719–e28719. <https://doi.org/10.1371/journal.pone.0028719>
- Agarwal D, Sandor C, Volpato V, et al (2020) A single-cell atlas of the human substantia nigra reveals cell-specific pathways associated with neurological disorders. *Nat Commun* 11:1–11. <https://doi.org/10.1038/s41467-020-17876-0>
- Aguila J, Cheng S, Kee N, et al (2021) Spatial RNA Sequencing Identifies Robust Markers of Vulnerable and Resistant Human Midbrain Dopamine Neurons and Their Expression in Parkinson’s Disease. *Front. Mol. Neurosci.* 14:699562. <https://doi.org/10.3389/fnmol.2021.699562>
- Alavian KN, Jeddi S, Naghipour SI, et al (2014) The lifelong maintenance of mesencephalic dopaminergic neurons by Nurr1 and engrailed. *J Biomed Sci* 21:27. <https://doi.org/10.1186/1423-0127-21-27>
- Anders S, Pyl PT, Huber W (2015) HTSeq--a Python framework to work with high-throughput sequencing data. *Bioinformatics* 31:166–9. <https://doi.org/10.1093/bioinformatics/btu638>
- Arenas E, Denham M, Villaescusa JC (2015) How to make a midbrain dopaminergic neuron. *Development* 142:1918–36. <https://doi.org/10.1242/dev.097394>
- Ascherio A, Schwarzschild MA (2016) The epidemiology of Parkinson’s disease: risk factors and prevention. *Lancet Neurol* 15:1257–1272.

[https://doi.org/10.1016/S1474-4422\(16\)30230-7](https://doi.org/10.1016/S1474-4422(16)30230-7)

Ayton S, Lei P (2014) Nigral iron elevation is an invariable feature of Parkinson's disease and is a sufficient cause of neurodegeneration. *Biomed Res Int* 2014:581256. <https://doi.org/10.1155/2014/581256>

Baek S, Choi H, Kim J (2014) Ebf3-miR218 regulation is involved in the development of dopaminergic neurons. *Brain Res* 1587:23–32.

<https://doi.org/10.1016/j.brainres.2014.08.059>

Bissonette GB, Roesch MR (2016) Development and function of the midbrain dopamine system: what we know and what we need to. *Genes Brain Behav* 15:62–73.

<https://doi.org/10.1111/gbb.12257>.

Blaudin de Thé F-X, Rekaik H, Prochiantz A, et al (2016) Neuroprotective Transcription Factors in Animal Models of Parkinson Disease. *Neural Plast* 2016:1–11.

<https://doi.org/10.1155/2016/6097107>

Blighe K, Rana S, Lewis M (2019) EnhancedVolcano: Publication-ready volcano plots with enhanced colouring and labeling

Bolger AM, Lohse M, Usadel B (2014) Trimmomatic: a flexible trimmer for Illumina sequence data. *Bioinformatics* 30:2114–20.

<https://doi.org/10.1093/bioinformatics/btu170>

Booth HDE, Wessely F, Connor-Robson N, et al (2019) RNA sequencing reveals MMP2 and TGFB1 downregulation in LRRK2 G2019S Parkinson's iPSC-derived astrocytes. *Neurobiol Dis* 129:56–66. <https://doi.org/10.1016/j.nbd.2019.05.006>

Borrageiro G, Haylett W, Seedat S, et al (2018) A review of genome-wide transcriptomics studies in Parkinson's disease. *Eur J Neurosci* 47:1–16.

<https://doi.org/10.1111/ejn.13760>

Brazel DM, Jiang Y, Hughey JM, et al (2019) Exome Chip Meta-analysis Fine Maps Causal Variants and Elucidates the Genetic Architecture of Rare Coding Variants in Smoking and Alcohol Use. *Biol Psychiatry* 85:946–955.

<https://doi.org/10.1016/j.biopsych.2018.11.024>

Carvalho AN, Marques C, Rodrigues E, et al (2013) Ubiquitin–Proteasome System Impairment and MPTP-Induced Oxidative Stress in the Brain of C57BL/6 Wild-type and GSTP Knockout Mice. *Mol Neurobiol* 47:662–672.

<https://doi.org/10.1007/s12035-012-8368-4>

Chomczynski P, Sacchi N (2006) The single-step method of RNA isolation by acid guanidinium thiocyanate–phenol–chloroform extraction: twenty-something years on. *Nat Protoc* 1:581–585. <https://doi.org/10.1038/nprot.2006.83>

Consortium SWG of the PG (2014) Biological insights from 108 schizophrenia-associated genetic loci. *Nature* 511:421–427. <https://doi.org/10.1038/nature13595>

Cook C, Petrucelli L (2009) A critical evaluation of the ubiquitin-proteasome system in Parkinson's disease. *Biochim Biophys Acta* 1792:664–75.

<https://doi.org/10.1016/j.bbadis.2009.01.012>

Cotzias GC (1968) L-Dopa for Parkinsonism. *N Engl J Med* 278:630.

<https://doi.org/10.1056/NEJM196803142781127>

Domanskyi A, Alter H, Vogt MA, et al (2014) Transcription factors Foxa1 and Foxa2 are required for adult dopamine neurons maintenance. *Front Cell Neurosci* 8:275.

<https://doi.org/10.3389/fncel.2014.00275>

Doucet-Beaupré H, Gilbert C, Profes MS, et al (2016) Lmx1a and Lmx1b regulate

- mitochondrial functions and survival of adult midbrain dopaminergic neurons. Proc Natl Acad Sci 113:E4387–E4396. <https://doi.org/10.1073/pnas.1520387113>
- Drinkut A, Tillack K, Meka DP, et al (2016) Ret is essential to mediate GDNF's neuroprotective and neuroregenerative effect in a Parkinson disease mouse model. Cell Death Dis 7:e2359. <https://doi.org/10.1038/cddis.2016.263>
- Evangelou E, Gao H, Chu C, et al (2019) New alcohol-related genes suggest shared genetic mechanisms with neuropsychiatric disorders. Nat Hum Behav 3:950–961. <https://doi.org/10.1038/s41562-019-0653-z>
- Fernández-Santiago R, Carballo-Carbajal I, Castellano G, et al (2015) Aberrant epigenome in iPSC-derived dopaminergic neurons from Parkinson's disease patients. EMBO Mol Med 7:1529–1546. <https://doi.org/10.15252/emmm.201505439>
- Greene JG (2012) Current status and future directions of gene expression profiling in Parkinson's disease. Neurobiol Dis 45:76–82. <https://doi.org/10.1016/j.nbd.2010.10.022>
- Greenwood TA, Lazzeroni LC, Maihofer AX, et al (2019) Genome-wide Association of Endophenotypes for Schizophrenia From the Consortium on the Genetics of Schizophrenia (COGS) Study. JAMA psychiatry. <https://doi.org/10.1001/jamapsychiatry.2019.2850>
- Grima B, Lamouroux A, Boni C, et al (1987) A single human gene encoding multiple tyrosine hydroxylases with different predicted functional characteristics. Nature 326:707–711. <https://doi.org/10.1038/326707a0>
- Gundersen HJ, Jensen EB (1987) The efficiency of systematic sampling in stereology and its prediction. J Microsc 147:229–63. <https://doi.org/10.1111/j.1365->

2818.1987.tb02837.x

Guo Y, Ma J, Huang H, et al (2022) Defining Specific Cell States of MPTP-Induced

Parkinson's Disease by Single-Nucleus RNA Sequencing. *Int J Mol Sci* 23:.

<https://doi.org/10.3390/ijms231810774>

Hao Y, Hao S, Andersen-Nissen E, et al (2021) Integrated analysis of multimodal

single-cell data. *Cell* 184:3573-3587.e29. <https://doi.org/10.1016/j.cell.2021.04.048>

Hegarty S V., Sullivan AM, O'Keeffe GW (2013) Midbrain dopaminergic neurons: A

review of the molecular circuitry that regulates their development. *Dev Biol*

379:123–138. <https://doi.org/10.1016/j.ydbio.2013.04.014>

Hirsch EC, Vyas S, Hunot S (2012) Neuroinflammation in Parkinson's disease.

*Parkinsonism Relat Disord* 18:S210–S212. [https://doi.org/10.1016/S1353-8020\(11\)70065-7](https://doi.org/10.1016/S1353-8020(11)70065-7)

Hoekstra EJ, von Oerthel L, van der Heide LP, et al (2013a) *Lmx1a* Encodes a Rostral

Set of Mesodiencephalic Dopaminergic Neurons Marked by the Wnt/B-Catenin

Signaling Activator R-spondin 2. *PLoS One* 8:e74049.

<https://doi.org/10.1371/journal.pone.0074049>

Hoekstra EJ, von Oerthel L, van der Linden AJA, et al (2013b) *Lmx1a* is an activator of

*Rgs4* and *Grb10* and is responsible for the correct specification of rostral and

medial mdDA neurons. *Eur J Neurosci* 37:23–32. <https://doi.org/10.1111/ejn.12022>

Hornykiewicz O (2010) A brief history of levodopa. *J Neurol* 257:S249-52.

<https://doi.org/10.1007/s00415-010-5741-y>

Huang DW, Sherman BT, Lempicki RA (2009a) Bioinformatics enrichment tools: paths

toward the comprehensive functional analysis of large gene lists. *Nucleic Acids Res*

37:1–13. <https://doi.org/10.1093/nar/gkn923>

Huang DW, Sherman BT, Lempicki RA (2009b) Systematic and integrative analysis of large gene lists using DAVID bioinformatics resources. *Nat Protoc* 4:44–57.  
<https://doi.org/10.1038/nprot.2008.211>

Infante J, Prieto C, Sierra M, et al (2016) Comparative blood transcriptome analysis in idiopathic and LRRK2 G2019S–associated Parkinson’s disease. *Neurobiol Aging* 38:214.e1–214.e5. <https://doi.org/10.1016/j.neurobiolaging.2015.10.026>

Iwata N, Kobayashi K, Sasaoka T, et al (1992) Structure of the mouse tyrosine hydroxylase gene. *Biochem Biophys Res Commun* 182:348–354.  
[https://doi.org/10.1016/S0006-291X\(05\)80151-2](https://doi.org/10.1016/S0006-291X(05)80151-2)

Jackson-Lewis V, Przedborski S (2007) Protocol for the MPTP mouse model of Parkinson’s disease. *Nat Protoc* 2:141–151. <https://doi.org/10.1038/nprot.2006.342>  
Jacobs FMJ, van der Linden AJA, Wang Y, et al (2009) Identification of Dlk1, Ptpru and Klhl1 as novel Nurr1 target genes in meso-diencephalic dopamine neurons. *Development* 136:2363–2373. <https://doi.org/10.1242/dev.037556>

Jansen PR, Watanabe K, Stringer S, et al (2019) Genome-wide analysis of insomnia in 1,331,010 individuals identifies new risk loci and functional pathways. *Nat Genet* 51:394–403. <https://doi.org/10.1038/s41588-018-0333-3>

Keo A, Mahfouz A, Ingrassia AMT, et al (2020) Transcriptomic signatures of brain regional vulnerability to Parkinson’s disease. *Commun Biol* 3:101.  
<https://doi.org/10.1038/s42003-020-0804-9>

Kim D, Pertea G, Trapnell C, et al (2013) TopHat2: accurate alignment of transcriptomes in the presence of insertions, deletions and gene fusions. *Genome*

Biol 14:R36. <https://doi.org/10.1186/gb-2013-14-4-r36>

Kogenaru S, Qing Y, Guo Y, Wang N (2012) RNA-seq and microarray complement each other in transcriptome profiling. BMC Genomics 13:629.  
<https://doi.org/10.1186/1471-2164-13-629>

Kolde R (2012) Pheatmap: pretty heatmaps. R Packag 61:617

Kouwenhoven WM, Von Oerthel L, Smidt MP (2017) Pitx3 and En1 determine the size and molecular programming of the dopaminergic neuronal pool. PLoS One 12:1–18. <https://doi.org/10.1371/journal.pone.0182421>

Kramer ER, Liss B (2015) GDNF-Ret signaling in midbrain dopaminergic neurons and its implication for Parkinson disease. FEBS Lett 589:3760–3772.  
<https://doi.org/10.1016/j.febslet.2015.11.006>

Laguna A, Schintu N, Nobre A, et al (2015) Dopaminergic control of autophagic-lysosomal function implicates Lmx1b in Parkinson's disease. Nat Neurosci 18:826–835. <https://doi.org/10.1038/nn.4004>

Lane JM, Liang J, Vlasac I, et al (2017) Genome-wide association analyses of sleep disturbance traits identify new loci and highlight shared genetics with neuropsychiatric and metabolic traits. Nat Genet 49:274–281.  
<https://doi.org/10.1038/ng.3749>

Lee HS, Bae EJ, Yi SH, et al (2010) Foxa2 and Nurr1 synergistically yield A9 nigral dopamine neurons exhibiting improved differentiation, function, and cell survival. Stem Cells 28:501–512. <https://doi.org/10.1002/stem.294>

Lei Z, Jiang Y, Li T, et al (2011) Signaling of Glial Cell Line-Derived Neurotrophic Factor and Its Receptor GFR $\alpha$ 1 Induce Nurr1 and Pitx3 to Promote Survival of Grafted

Midbrain-Derived Neural Stem Cells in a Rat Model of Parkinson Disease. J Neuropathol Exp Neurol 70:736–747.

<https://doi.org/10.1097/NEN.0b013e31822830e5>

Lewis DA, Melchitzky DS, Haycock JW (1993) Four isoforms of tyrosine hydroxylase are expressed in human brain. Neuroscience 54:477–492.

[https://doi.org/10.1016/0306-4522\(93\)90267-J](https://doi.org/10.1016/0306-4522(93)90267-J)

Li H, Handsaker B, Wysoker A, et al (2009) The Sequence Alignment/Map format and SAMtools. Bioinformatics 25:2078–2079.

<https://doi.org/10.1093/bioinformatics/btp352>

Li Z, Wu H (2019) TOAST: improving reference-free cell composition estimation by cross-cell type differential analysis. Genome Biol 20:190.

<https://doi.org/10.1186/s13059-019-1778-0>

Li Z, Wu Z, Jin P, Wu H (2019) Dissecting differential signals in high-throughput data from complex tissues. Bioinformatics 35:3898–3905.

<https://doi.org/10.1093/bioinformatics/btz196>

Lin W, Metzakopian E, Mavromatakis YE, et al (2009) Foxa1 and Foxa2 function both upstream of and cooperatively with Lmx1a and Lmx1b in a feedforward loop promoting mesodiencephalic dopaminergic neuron development. Dev Biol 333:386–396. <https://doi.org/10.1016/j.ydbio.2009.07.006>

Love MI, Huber W, Anders S (2014) Moderated estimation of fold change and dispersion for RNA-seq data with DESeq2. Genome Biol 15:550.

<https://doi.org/10.1186/s13059-014-0550-8>

Malone JH, Oliver B (2011) Microarrays, deep sequencing and the true measure of the

- transcriptome. *BMC Biol* 9:34. <https://doi.org/10.1186/1741-7007-9-34>
- Mancarci BO, Toker L, Tripathy SJ, et al (2017) Cross-laboratory analysis of brain cell type transcriptomes with applications to interpretation of bulk tissue data. *eNeuro* 4:. <https://doi.org/10.1523/ENEURO.0212-17.2017>
- Maraganore DM, Lesnick TG, Elbaz A, et al (2004) UCHL1 is a Parkinson's disease susceptibility gene. *Ann Neurol* 55:512–521. <https://doi.org/10.1002/ana.20017>
- Matoba N, Akiyama M, Ishigaki K, et al (2019) GWAS of smoking behaviour in 165,436 Japanese people reveals seven new loci and shared genetic architecture. *Nat Hum Behav* 3:471–477. <https://doi.org/10.1038/s41562-019-0557-y>
- Miller RM, Federoff HJ (2005) Altered Gene Expression Profiles Reveal Similarities and Differences Between Parkinson Disease and Model Systems. *Neurosci* 11:539–549. <https://doi.org/10.1177/1073858405278330>
- Moni MA, Rana HK, Islam MB, et al (2019) A computational approach to identify blood cell-expressed Parkinson's disease biomarkers that are coordinately expressed in brain tissue. *Comput Biol Med* 113:103385.  
<https://doi.org/10.1016/j.combiomed.2019.103385>
- Murakami M, Ichihara M, Sobue S, et al (2007) RET signaling-induced SPHK1 gene expression plays a role in both GDNF-induced differentiation and MEN2-type oncogenesis. *J Neurochem* 102:1585–1594. <https://doi.org/10.1111/j.1471-4159.2007.04673.x>
- Murakami M, Ito H, Hagiwara K, et al (2011) Sphingosine kinase 1/S1P pathway involvement in the GDNF-induced GAP43 transcription. *J Cell Biochem* 112:3449–3458. <https://doi.org/10.1002/jcb.23275>

Nair-Roberts RG, Chatelain-Badie SD, Benson E, et al (2008) Stereological estimates of dopaminergic, GABAergic and glutamatergic neurons in the ventral tegmental area, substantia nigra and retrorubral field in the rat. *Neuroscience* 152:1024–31.  
<https://doi.org/10.1016/j.neuroscience.2008.01.046>

Nalls MA, Blauwendraat C, Vallerga CL, et al (2019) Identification of novel risk loci, causal insights, and heritable risk for Parkinson's disease: a meta-analysis of genome-wide association studies. *Lancet Neurol* 18:1091–1102.  
[https://doi.org/10.1016/S1474-4422\(19\)30320-5](https://doi.org/10.1016/S1474-4422(19)30320-5)

Park J, Kim Y, Chung J (2009) Mitochondrial dysfunction and Parkinson's disease genes: Insights from Drosophila. *Dis Model Mech* 2:336–340.  
<https://doi.org/10.1242/dmm.003178>

Parkinson JD (1817) An Essay on the Shaking Palsy. London Whittingham Rowl  
Sherwood, Neely, Jones 14:223–236. <https://doi.org/10.1176/jnp.14.2.223>

Peng C, Aron L, Klein R, et al (2011) Pitx3 Is a Critical Mediator of GDNF-Induced BDNF Expression in Nigrostriatal Dopaminergic Neurons. *J Neurosci* 31:12802–12815. <https://doi.org/10.1523/JNEUROSCI.0898-11.2011>

Pifl C, Rajput A, Reither H, et al (2014) Is Parkinson's disease a vesicular dopamine storage disorder? Evidence from a study in isolated synaptic vesicles of human and nonhuman primate striatum. *J Neurosci* 34:8210–8218.

<https://doi.org/10.1523/JNEUROSCI.5456-13.2014>

Prakash N, Wurst W (2006) Genetic networks controlling the development of midbrain dopaminergic neurons. *J Physiol* 575:403–410.  
<https://doi.org/10.1113/jphysiol.2006.113464>

Riley BE, Gardai SJ, Emig-Agius D, et al (2014) Systems-Based Analyses of Brain Regions Functionally Impacted in Parkinson's Disease Reveals Underlying Causal Mechanisms. PLoS One 9:e102909. <https://doi.org/10.1371/journal.pone.0102909>

Saeed U, Karunakaran S, Meka DP, et al (2009) Redox Activated MAP Kinase Death Signaling Cascade Initiated by ASK1 is not Activated in Female Mice Following MPTP: Novel Mechanism of Neuroprotection. Neurotox Res 16:116–126. <https://doi.org/10.1007/s12640-009-9058-5>

Schapira AH V., Cooper JM, Dexter D, et al (1990) Mitochondrial Complex I Deficiency in Parkinson's Disease. J Neurochem 54:823–827. <https://doi.org/10.1111/j.1471-4159.1990.tb02325.x>

Sherman MY, Goldberg AL (2001) Cellular Defenses against Unfolded Proteins: A Cell Biologist Thinks about Neurodegenerative Diseases. Neuron 29:15–32. [https://doi.org/10.1016/S0896-6273\(01\)00177-5](https://doi.org/10.1016/S0896-6273(01)00177-5)

Sherva R, Wang Q, Kranzler H, et al (2016) Genome-wide Association Study of Cannabis Dependence Severity, Novel Risk Variants, and Shared Genetic Risks. JAMA psychiatry 73:472–480. <https://doi.org/10.1001/jamapsychiatry.2016.0036>

Simon HH, Bhatt L, Gherbassi D, et al (2003) Midbrain dopaminergic neurons: determination of their developmental fate by transcription factors. Ann N Y Acad Sci 991:36–47

Simon HH, Saueressig H, Wurst W, et al (2001) Fate of Midbrain Dopaminergic Neurons Controlled by the Engrailed Genes. J Neurosci 21:3126 LP – 3134. <https://doi.org/10.1523/JNEUROSCI.21-09-03126.2001>

Simunovic F, Yi M, Wang Y, et al (2009) Gene expression profiling of substantia nigra

- dopamine neurons: further insights into Parkinson's disease pathology. *Brain* 132:1795–1809. <https://doi.org/10.1093/brain/awn323>
- Smidt MP (2017) Molecular Programming of Mesodiencephalic Dopaminergic Neuronal Subsets. *Front Neuroanat* 11:59. <https://doi.org/10.3389/fnana.2017.00059>
- Sofic E, Riederer P, Heinsen H, et al (1988) Increased iron (III) and total iron content in post mortem substantia nigra of parkinsonian brain. *J Neural Transm* 74:199–205. <https://doi.org/10.1007/BF01244786>
- Soreq L, Salomonis N, Guffanti A, et al (2015) Whole transcriptome RNA sequencing data from blood leukocytes derived from Parkinson's disease patients prior to and following deep brain stimulation treatment. *Genomics Data* 3:57–60. <https://doi.org/10.1016/j.gdata.2014.11.009>
- Spada J, Scholz M, Kirsten H, et al (2016) Genome-wide association analysis of actigraphic sleep phenotypes in the LIFE Adult Study. *J Sleep Res* 25:690–701. <https://doi.org/10.1111/jsr.12421>
- Stefanis L (2012) α-Synuclein in Parkinson's disease. *Cold Spring Harb Perspect Med* 2:a009399–a009399. <https://doi.org/10.1101/cshperspect.a009399>
- Sutherland GT, Matigian NA, Chalk AM, et al (2009) A Cross-Study Transcriptional Analysis of Parkinson's Disease. *PLoS One* 4:e4955. <https://doi.org/10.1371/journal.pone.0004955>
- Szklarczyk D, Gable AL, Lyon D, et al (2019) STRING v11: protein-protein association networks with increased coverage, supporting functional discovery in genome-wide experimental datasets. *Nucleic Acids Res* 47:D607–D613. <https://doi.org/10.1093/nar/gky1131>

Thuret S, Bhatt L, O'Leary DD., Simon HH (2004) Identification and developmental analysis of genes expressed by dopaminergic neurons of the substantia nigra pars compacta. *Mol Cell Neurosci* 25:394–405.

<https://doi.org/10.1016/j.mcn.2003.11.004>

Tiklová K, Gillberg L, Volakakis N, et al (2021) Disease Duration Influences Gene Expression in Neuromelanin-Positive Cells From Parkinson's Disease Patients. *Front. Mol. Neurosci.* 14:763777. <https://doi.org/10.3389/fnmol.2021.763777>

Tong W, Zhang K, Yao H, et al (2022) Transcriptional Profiling Reveals Brain Region-Specific Gene Networks Regulated in Exercise in a Mouse Model of Parkinson's Disease. *Front. Aging Neurosci.* 14:891644.

<http://doi.org/10.3389/fnagi.2022.891644>.

Trapnell C, Roberts A, Goff L, et al (2012) Differential gene and transcript expression analysis of RNA-seq experiments with TopHat and Cufflinks. *Nat Protoc* 7:562–78.

<https://doi.org/10.1038/nprot.2012.016>

van den Hurk M, Lau S, Marchetto MC, et al (2022) Druggable transcriptomic pathways revealed in Parkinson's patient-derived midbrain neurons. *npj Park Dis* 8:134.

<https://doi.org/10.1038/s41531-022-00400-0>

Veenvliet J V., dos Santos MTMA, Kouwenhoven WM, et al (2013) Specification of dopaminergic subsets involves interplay of En1 and Pitx3. *Development* 140:4116–4116. <https://doi.org/10.1242/dev.102731>

Villaescusa JC, Li B, Toledo EM, et al (2016) A PBX1 transcriptional network controls dopaminergic neuron development and is impaired in Parkinson's disease. *EMBO J* 35:1963–78. <https://doi.org/10.15252/embj.201593725>

Walter W, Sanchez-Cabo F, Ricote M (2015) GOplot: an R package for visually combining expression data with functional analysis. *Bioinformatics* 31:2912–2914.  
<https://doi.org/10.1093/bioinformatics/btv300>

West MJ, Slomianka L, Gundersen HJG (1991) Unbiased stereological estimation of the total number of neurons in the subdivisions of the rat hippocampus using the optical fractionator. *Anat Rec* 231:482–497. <https://doi.org/10.1002/ar.1092310411>

Yang W, Hao W, Meng Z, et al (2021) Molecular Regulatory Mechanism and Toxicology of Neurodegenerative Processes in MPTP/Probenecid-Induced Progressive Parkinson's Disease Mice Model Revealed by Transcriptome. *Mol Neurobiol* 58:603–616. <https://doi.org/10.1007/s12035-020-02128-5>

Zhang Y, James M, Middleton FA, Davis RL (2005) Transcriptional analysis of multiple brain regions in Parkinson's disease supports the involvement of specific protein processing, energy metabolism, and signaling pathways, and suggests novel disease mechanisms. *Am J Med Genet Part B Neuropsychiatr Genet* 137B:5–16.  
<https://doi.org/10.1002/ajmg.b.30195>

Zhou H, Polimanti R, Yang B-Z, et al (2017) Genetic Risk Variants Associated With Comorbid Alcohol Dependence and Major Depression. *JAMA psychiatry* 74:1234–1241. <https://doi.org/10.1001/jamapsychiatry.2017.3275>

Details of the patient samples are provided in Table 1.

Case No	Pathology	Sex	Age (years)	PMI	RIN	Treatment at time of death	Symptoms	Origin
Parkinson's disease								
3296	Transitional Lewy body disease + Grain Disease	M	81	24h	6.1	Sinemet + Sifrol + Comtan	akinesia + rigidity + gait disorders	Sporadic
4762	Diffuse Lewy body disease + Alz III lesions of Braak	F	83	12h	6.3	Modopar + Parlodel	akinesia + rigidity + gait disorders + slight cognitive impairment	Sporadic
7555	Diffuse Lewy body disease + Alz I lesions of Braak	F	80	23h	6.5	I-Dopa sensitive no information about treatment at time of death	akinesia + rigidity + gait disorders + slight cognitive impairment	Sporadic
7773	Diffuse Lewy body disease + Alz I lesions of Braak	M	80	18h	6.7	I-Dopa sensitive no information about treatment at time of death	akinesia + rigidity	GBA mutation E326K

Control								
4078	Control: presence of lesions of subacute and chronic ischemia of cortico- subcortical localization in moderate abundance	M	73	10h	6.3			
7197	Control with Braak stage II Alzheimer lesions + amyloid angiopathy	M	85	10h	6.5			
3549	Control right tonsil lesion	M	69	6h	7			

## Legends to Figures

**Fig.1 Differential gene expression in SNpc from MPTP mouse model of PD.** (A) A diagrammatic representation of SNpc dissection using coronal mouse midbrain sections. (B) Stereological analysis of tyrosine hydroxylase positive neurons in SNpc after 14 days of MPTP treatment (n=5). (C) Table depicting downregulation of genes specific to dopaminergic neurons in SNpc from 14 days MPTP treated mice. (D) and (E) The top 60 significantly differentially expressed genes after 1 day and 14 days of MPTP treatment, represented through heatmaps along with their  $\log_2$  fold change, respectively. (F) and (G) Volcano plots for differentially expressed genes in SNpc from 1 day and 14 days MPTP treated mice SNpc, respectively. (H) Venn diagram showing the overlap of the upregulated and downregulated genes between 1 day and 14 days MPTP treatment. Each dot represents an individual on the graphs. Comparisons between the groups were done using unpaired Student's t test. Data are presented as mean  $\pm$  SEM.

\* indicates p<0.05. Panel A was created originally using Adobe Illustrator. Heatmaps for panels D and E were generated using the R package, pheatmap 1.0.12. Volcano plots for panels F and G were generated using the R package, EnhancedVolcano 1.5.0. The Venn diagram in panel H was plotted using the online tool available at the url:

<http://bioinformatics.psb.ugent.be/webtools/Venn/>

**Fig. 2 Differentially expressed pathways enriched in SNpc from MPTP mouse model of PD.** (A) and (B) Bar diagrams for functional clusters derived using the Database for Annotation, Visualization and Integrated Discovery (DAVID) for significantly differentially expressed genes in 1 day and 14 days MPTP mouse model of PD, respectively. (C) and (D) Significantly differentially expressed genes and their

distribution into pathways hierarchically clustered according to functional categories along with the adjusted p values for 1 day and 14 days MPTP treated mice SNpc using circular plots, respectively. The innermost space represents the hierarchical clustering of the genes while the inner circle represents the  $\log_2$  fold change. (E) and (F) Chord diagrams for pathways depicting the significant genes that belong to at least three different pathways with their  $\log_2$  fold change for 1 day and 14 days MPTP treatment in mice, respectively. All the panels in this figure were generated using the R package, GOpplot 1.0.2

**Fig. 3 Differential gene expression in SNpc from human autopsy tissue samples.**  
(A) Graphical representation of human midbrain nuclei, namely central gray substance (CGS), red nucleus (RN), peri and retro rubral dopaminergic cell group (A8), substantia nigra pars compacta (SNpc: A9), ventral tegmental area (VTA: A10). (B) Differential gene expression in PD-from human autopsy tissue. The list displays the top 30-upregulated and downregulated genes in SNpc from PD autopsy tissue. The  $\log_2$  fold change and adjusted p value are also provided along with gene names. (C) Heatmap depicting differentially expressed genes in SNpc from human PD (D) Volcano plot representing the relative numbers of upregulated and downregulated genes. (E) Down-regulation of dopaminergic neuron markers in SNpc from autopsy tissue from PD patients. Panel A was created originally using Adobe Illustrator. Heatmap for panels C was generated using the R package, pheatmap 1.0.12. Volcano plots for panel D was generated using the R package, EnhancedVolcano 1.5.0

**Fig.4 Differentially expressed pathways enriched in SNpc from human autopsy tissue samples.** (A) Bar diagram of the differentially regulated functional clusters as

derived using DAVID from the significantly differentially expressed genes. (B) Circular plot for the significant genes enriched in pathways where the innermost space represents the hierarchical clustering of the genes while the inner circle represents the  $\log_2$  fold change. (C) Significantly differentially expressed genes that belong to at least two functional clusters and their  $\log_2$  fold change as represented using a chord diagram. (D) Table of genes that are involved in development, differentiation and maintenance of midbrain dopaminergic neurons with their  $\log_2$  fold change, p value and adjusted p value. Panels A–C were generated using the R package, GOplot 1.0.2

**Fig.5 Validation of down-regulation of genes involved in development and differentiation of midbrain DA neurons through qRT-PCR.** (A) Relative level of gene expression of *DAT*, *LMX1B*, *EN1*, *RET* and *GAP43* in on human autopsy SNpc as compared to age-matched controls as quantified using qRT-PCR. (B) Significant downregulation of *Th*, *Dat*, *Lmx1b*, *En1* and *Ret* but not of *Gap43* observed in SNpc from C57BL/6 mice treated with MPTP (s.c.) for 14 days. Each dot represents an individual on the graphs. Comparisons between the groups were done using unpaired Student's *t* test. n = 5-8; data has been presented as mean  $\pm$  SEM. \* indicates p<0.05

**Fig.6 *LMX1B-GFP* overexpression rescues SH-SY5Y from MPP<sup>+</sup> toxicity.** (A) String analysis of significantly perturbed midbrain dopaminergic neuron development, differentiation and maintenance genes. (B) Summary of role of genes involved in development and maintenance of SNpc dopaminergic neurons that were differentially expressed in human PD as derived from literature. (C) Immunoblot analysis of *LMX1B-GFP* in SH-SY5Y cells after transfection with *LMX1B-GFP* overexpression (*LMX1B* in pEGFP-N1) plasmid. (D) Quantification of TUNEL positive cells per field n = 28–30

images, 8–10 images taken per coverslip taken over three independent coverslips. (E) Representative images of SH-SY5Y neurons depicting the presence of GFP or *LMX1B*-GFP (green), TUNEL positive cells (red) and DAPI positive cells (blue) after overexpression of pEGFP-N1 (control plasmid) or *LMX1B* in pEGFP-N1 and treatment with 1 mM MPP<sup>+</sup>. Comparison between the groups was done using unpaired Student's *t* test. Data represented as mean ± SEM. One-way ANOVA with Tukey's test for multiple comparison was performed to compare the different groups. \* represents *p*<0.05. Scale bar represents 50 μm. Protein-protein associations that may result from co-differential expression of genes shown in panel A were drawn using the String database. Panel B was created originally using Adobe Illustrator.

**Figure. 1**

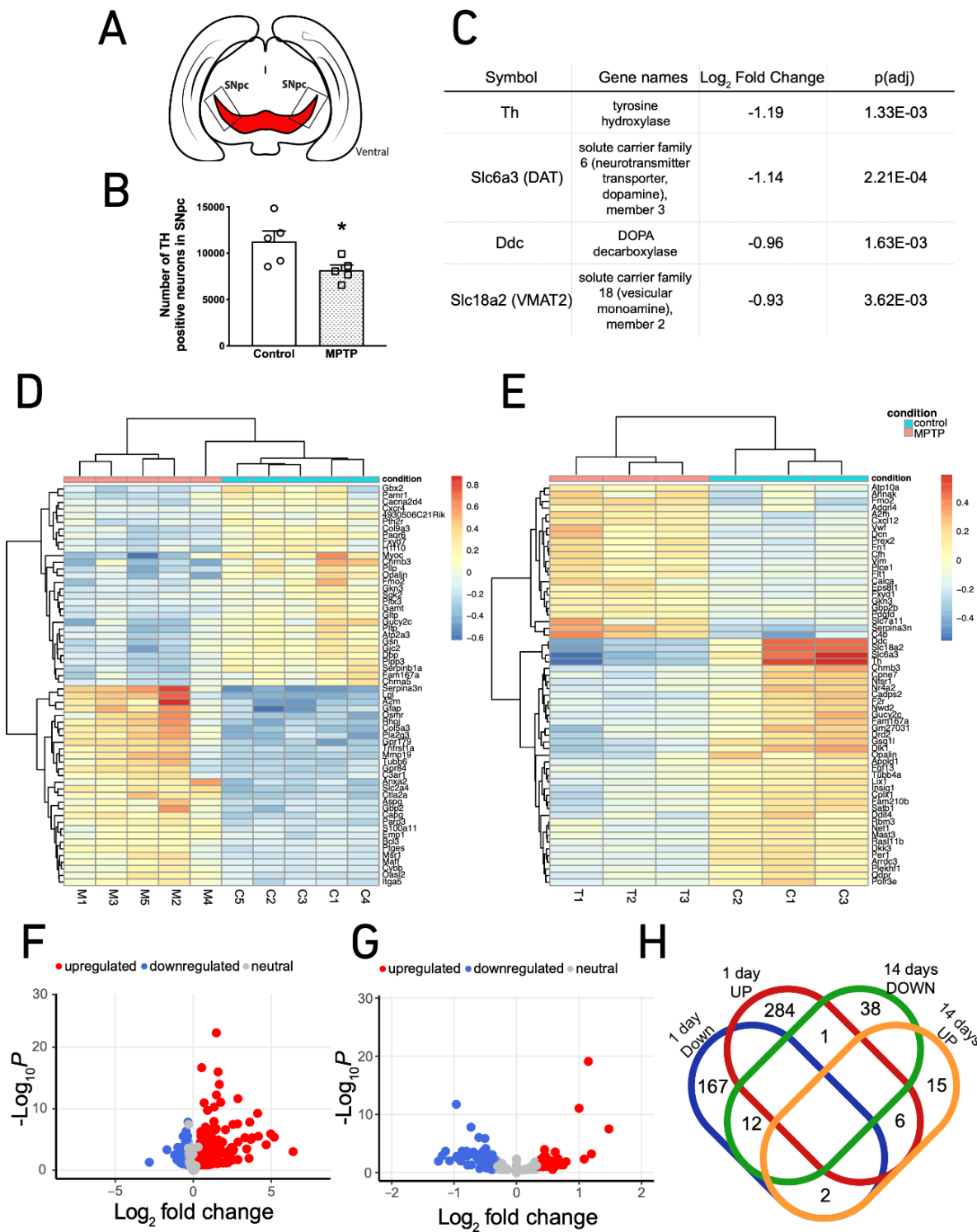


**Figure. 2**

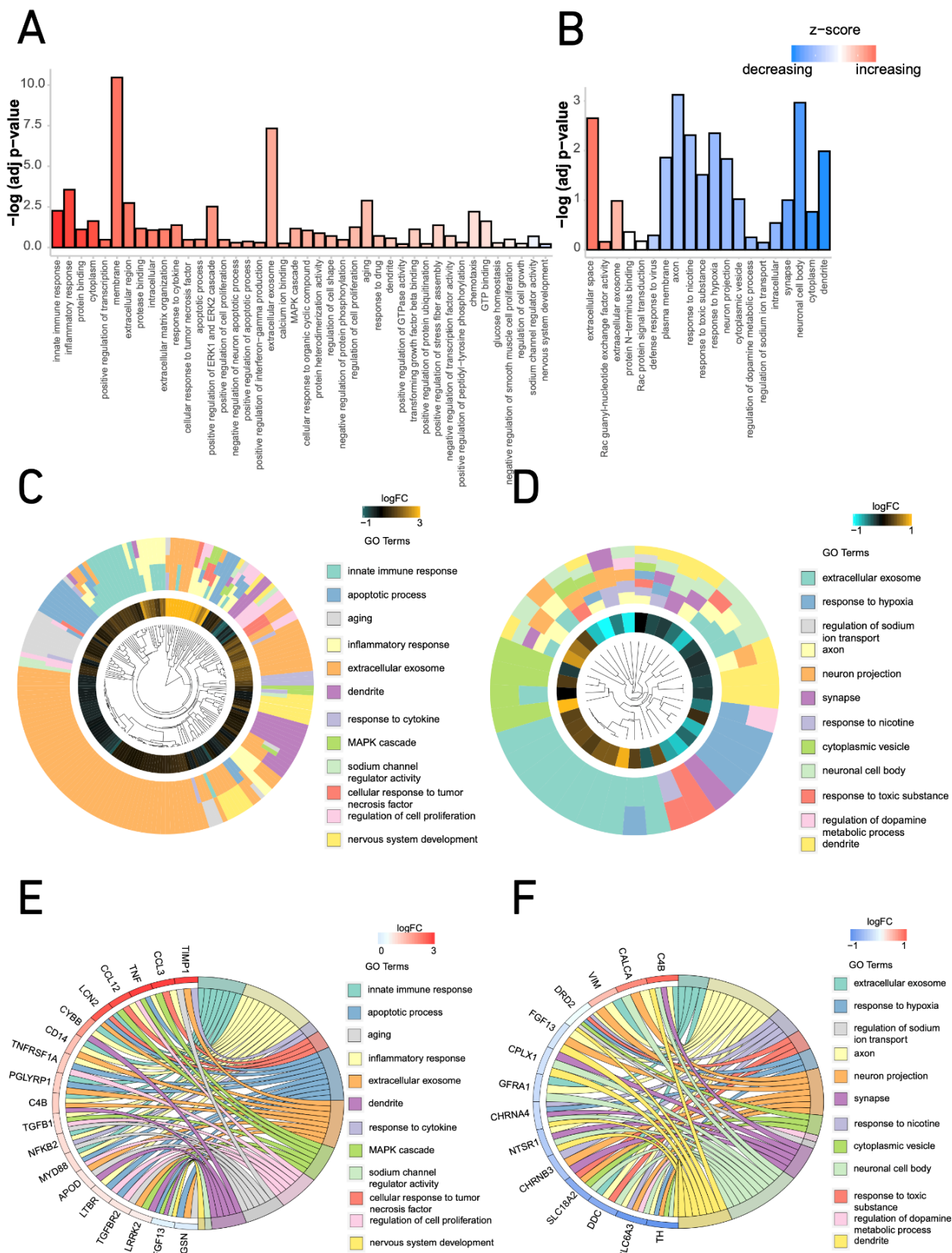


**Figure. 3**

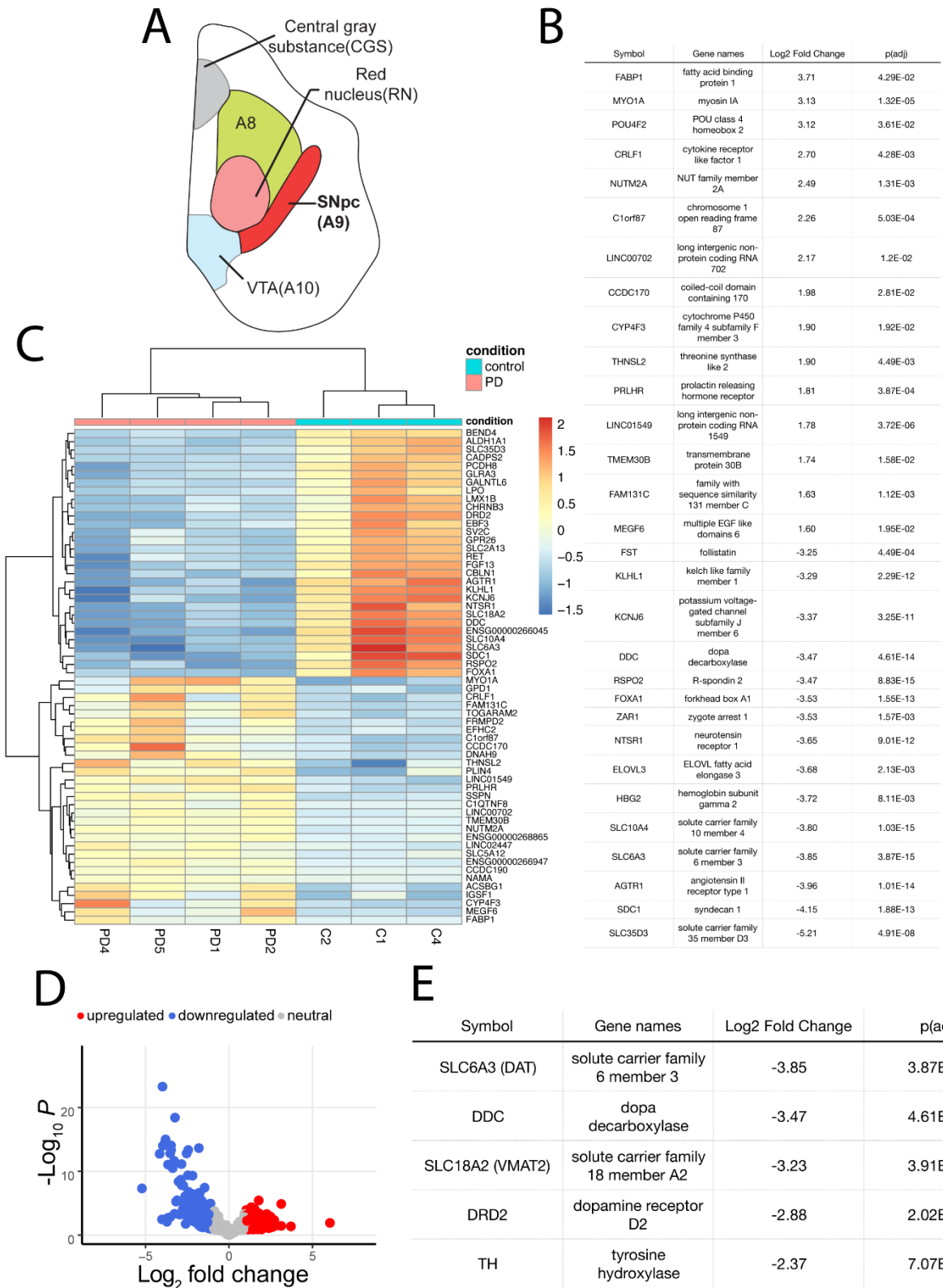


**Figure. 4**

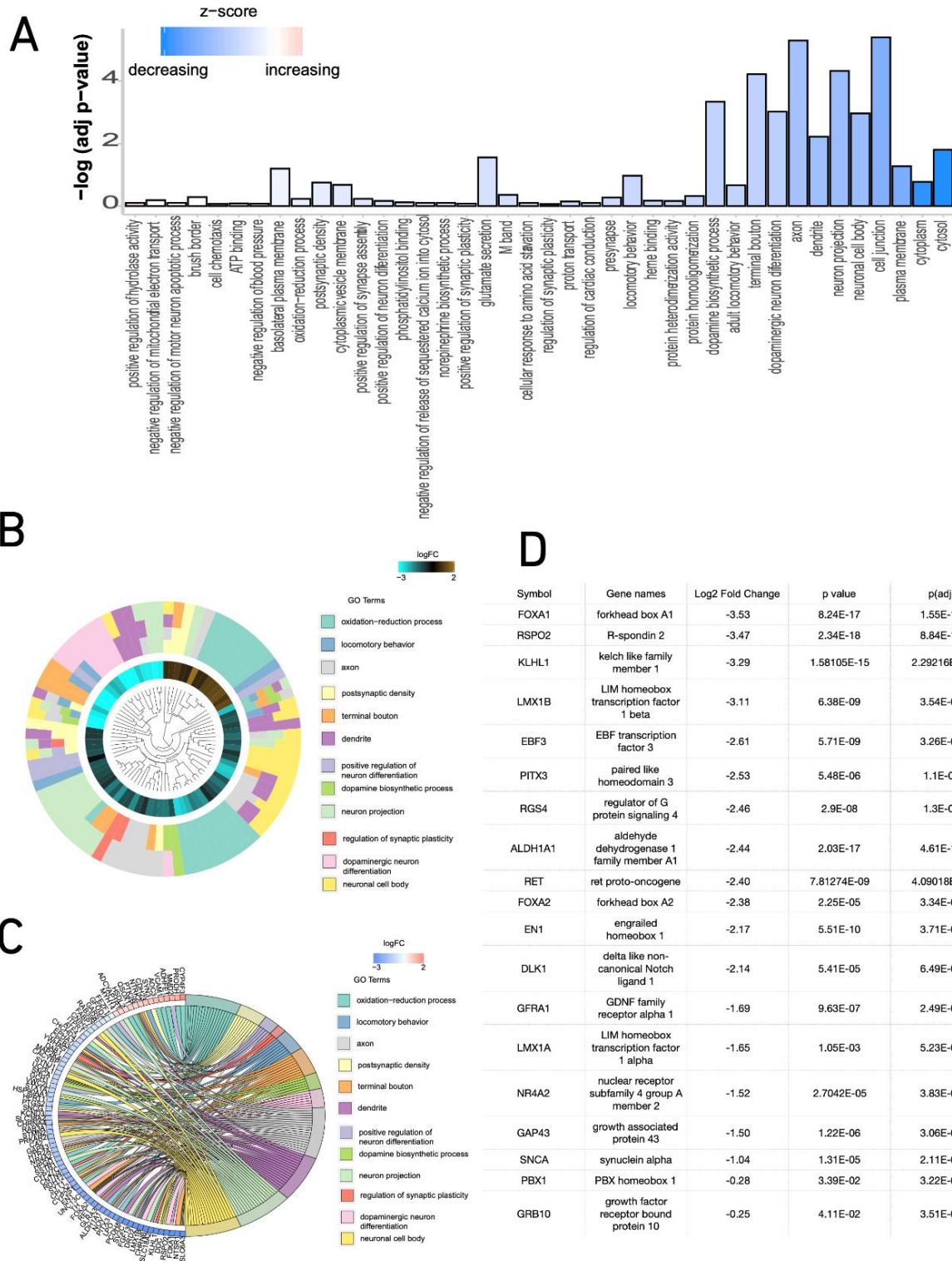
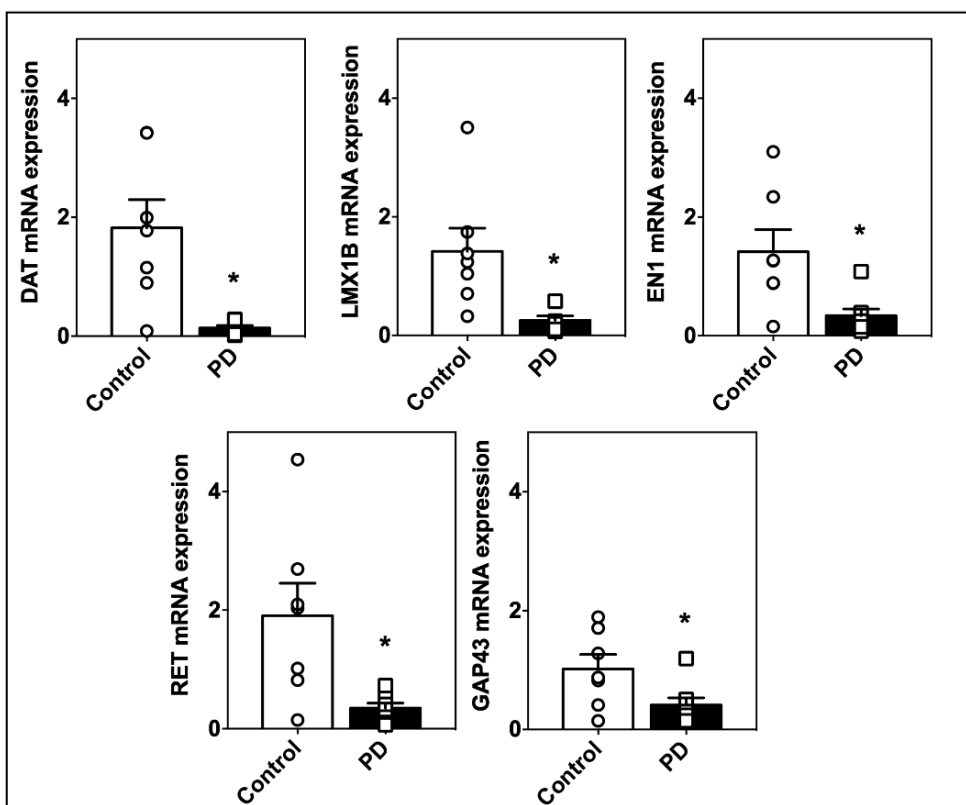


**Figure. 5**

A



B

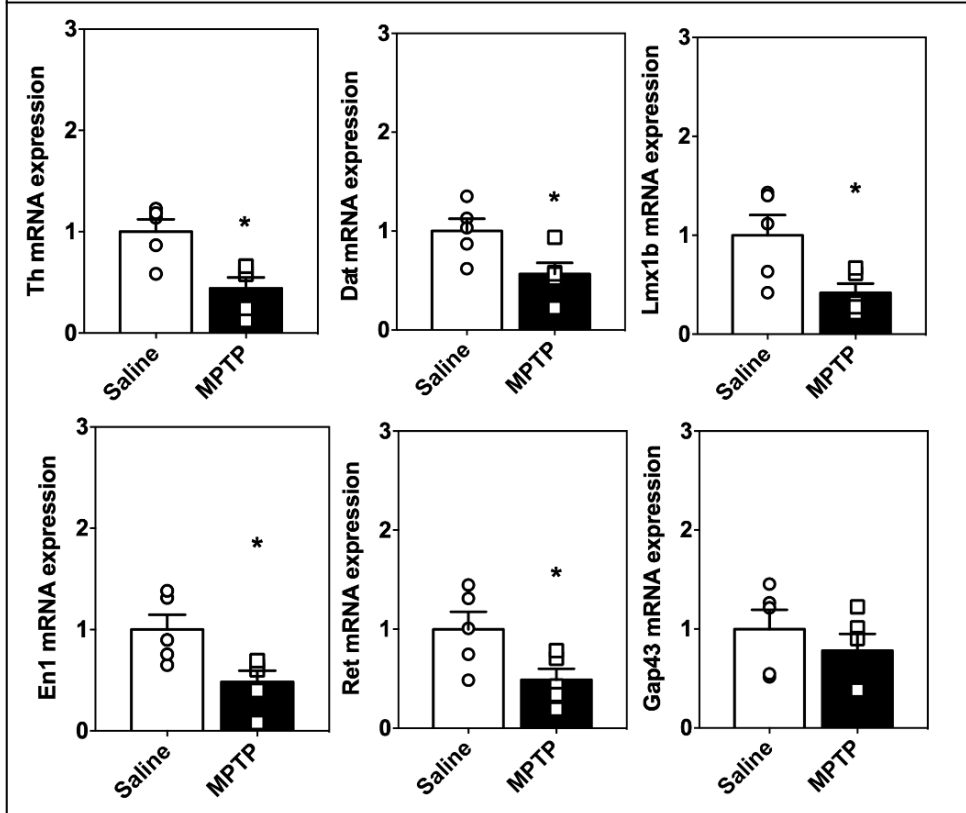
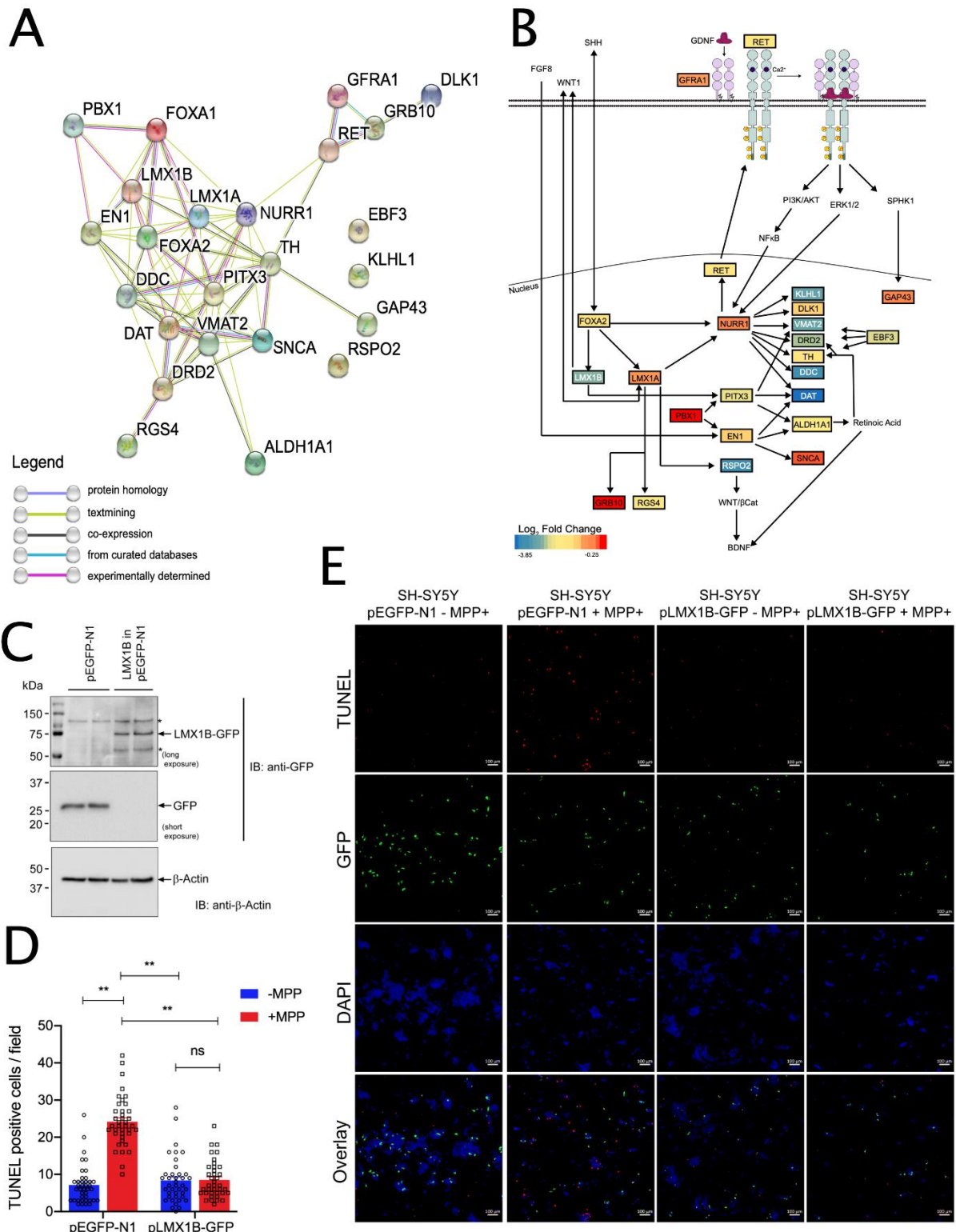


**Figure. 6**



## Supplementary data

A 24 HOURS MPTP TREATMENT	
Dopaminergic neurons	Th, Cdk5r2
Oligodendrocyte	Gamit, Pdlim2, Ppp1r14a, Mog, Olig2, Anln
Microglia (deactivation)	Slc2a5, Mafb, Lair1, Trim47, Fam111a, Slamf9, Atf3, Clec7a, Lcn2
Microglia (activation)	Ucp2, Parp14, Klf10, Myd88, Plek, Birc3, Lcp2, Runx1, Fcgr2b, Cd14, Cxcl16, Icam1, Soc3, Il1a, Tlr2, Plaur, Slc15a3, Gpr84, Ccl12, Tubb6, Trif, Cxcl10, Ccl4
Microglia	Tgfb2, Lcp1, Ctsz, Pros1, Tgfb1, Hk2, Gcnt1, Tcr4a, Phyhd1, Clec5a, Msn, Tbxas1, Cd68, Emp3, C3ar1, Tlr1, Lgals3, Ccl3
Astroglia	Pipp3, Lcat, Cldn10, Ntsr2, Slc7a10, Btbd17, Tlcd1, Abhd3, Pbxp1, Ppp1r3c, Wwtr1, Ccnd2, Scara3
B 14 DAYS MPTP TREATMENT	
Dopaminergic neurons	Dlk1, Cadps2, Slc6a3, Th, Nr4a2, Cpx1
Oligodendrocyte	None
Microglia (deactivation)	None
Microglia (activation)	None
Microglia	Cfh
Astroglia	None
C PARKINSON'S DISEASE (HUMAN PATIENTS)	
Dopaminergic neurons	CADPS2, CELF4, DLK1, ELAVL2, KLHL1, PCSK1, RET, SNCG, TH
Oligodendrocyte	None
Microglia (deactivation)	HPGD
Microglia (activation)	None
Microglia	None
Astroglia	ACSBG1, ADHFE1, ITGA7, PRODH, VCAM1

**Figure S1: Overlap of cell-type specific markers in differentially expressed genes.**

(A) Analysis of cell-type specific markers (Mancarci *et al.*, 2017) expressed among the differentially expressed genes 24 hours after a single dose of MPTP, (B) after 14 days of MPTP treatment, and (C) in human PD autopsy tissue.

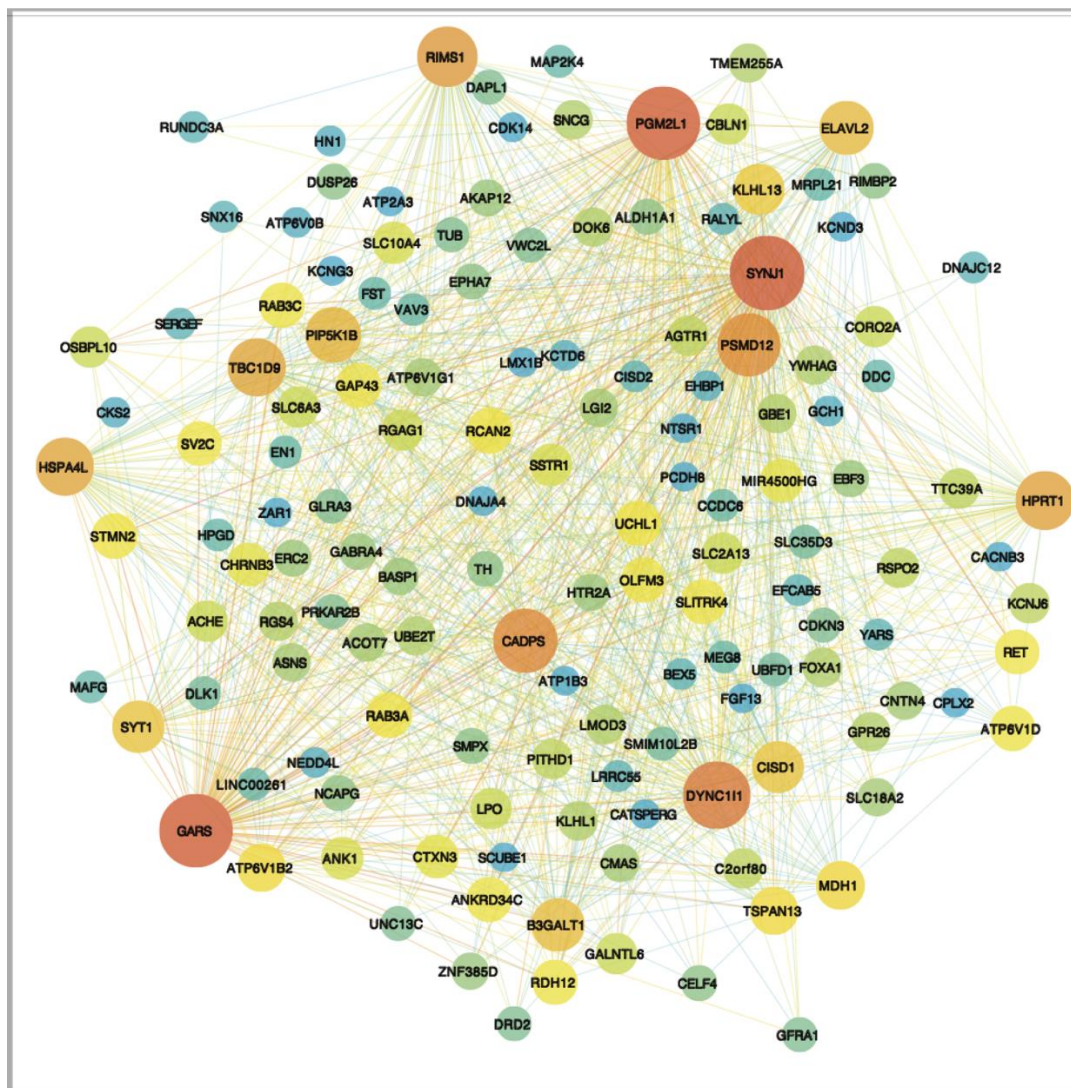


**Figure S2: Projected network analysis of significantly differentially expressed genes in PD autopsy tissue.**

Representation of complete network of genes perturbed in PD. A weight cut-off of 0.3 was placed which resulted in the network. The size of the node in the network refers to the degree of the node, i.e. number of connections the node has with other nodes. The degree of the node is also represented on a scale of red to blue, warmer colour referring to higher degree. Similarly, thickness of edge represents the weight of the

interaction which is also represented by the colour of the edge, warmer colours indicating higher weight of correlation. This figure was generated using Cytoscape.

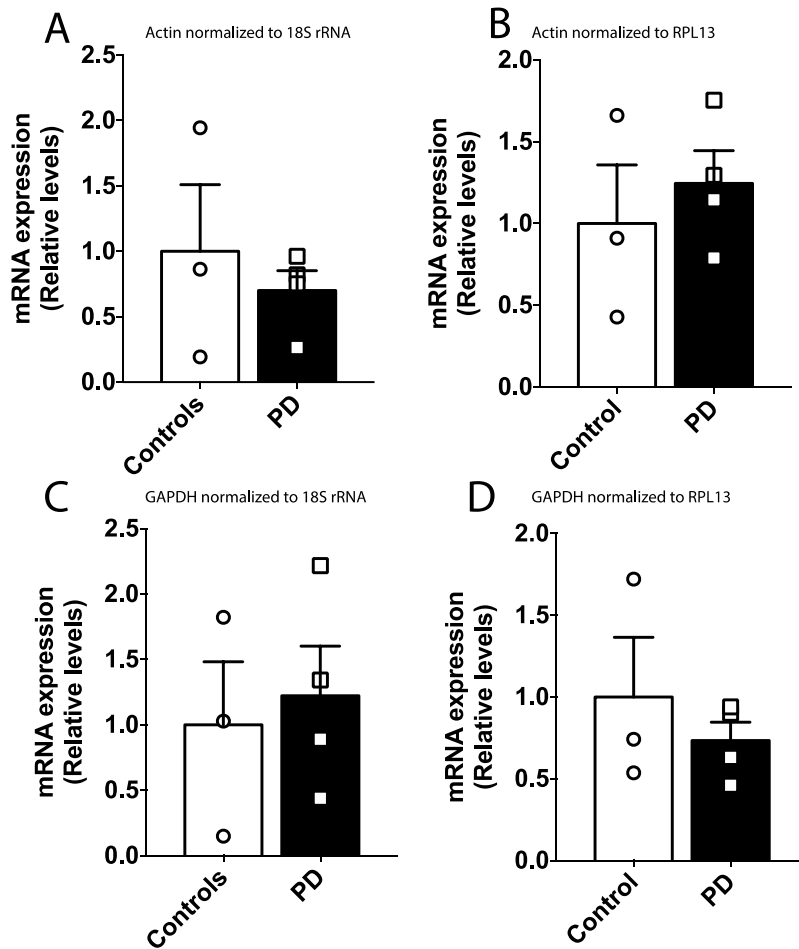


**Figure S3: Lack of differential gene expression of  $\beta$ -actin and GAPDH in human PD.** mRNA expression of  $\beta$ -actin does not change in PD human autopsy tissue as investigated through qRT-PCR when normalized to either 18S rRNA (A) or to RPL13 (B). The expression of GAPDH also does not alter in PD upon normalization to 18S rRNA (C) and RPL13 (D). Each point represents an individual sample. For controls n=3, for human PD samples, n=4. Unpaired, two-tailed Student' t test has been performed on

each control

Data has

SEM.

versus PD comparison.

been presented as mean  $\pm$

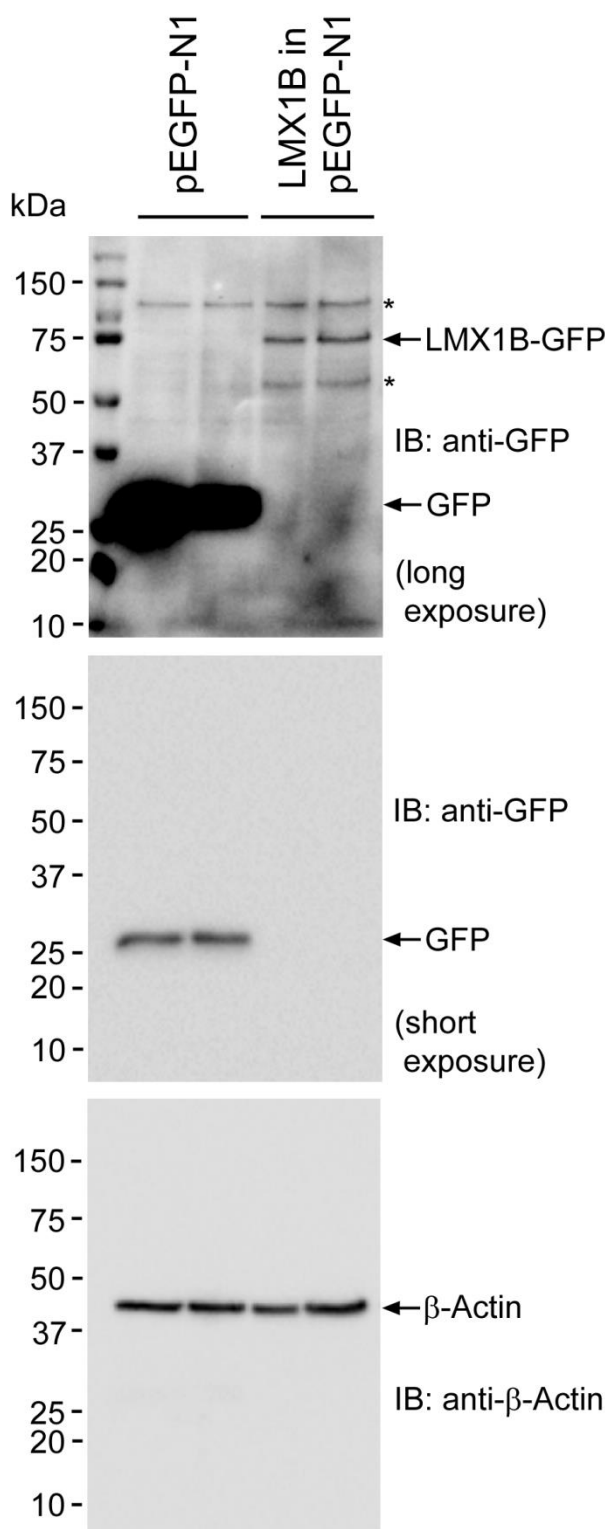


**Fig. S4. Full unedited immunoblots used for representation of Figure 6C.**

**Immunoblot analysis of pEGFP-N1 or LMX1B in pEGFP-N1 over expression in SH-SY5Y cells.** Lysates were prepared from SH-SY5Y cells after 48 hrs of transient transfection with pEGFP-N1 or LMX1B in pEGFP-N1 and subjected to SDS-PAGE followed by immunoblotting for anti-GFP antibody. Later, this blot was stripped and reprobed for  $\beta$ -actin as a loading control.

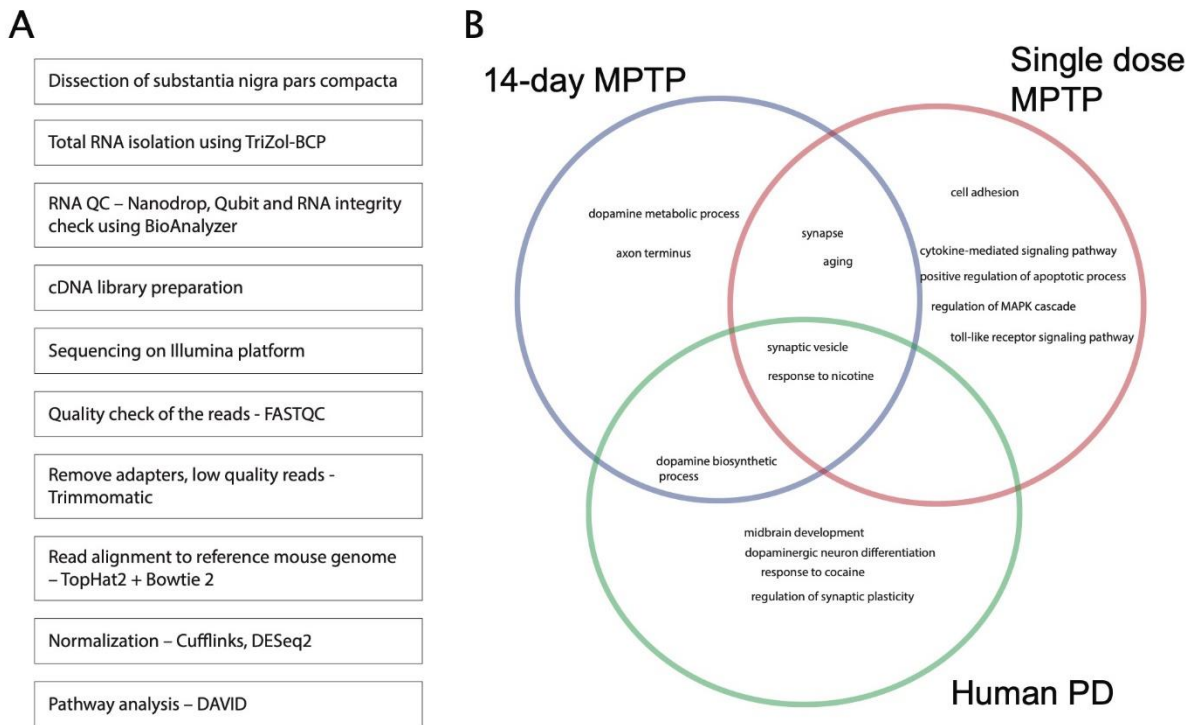


**Fig. S5. Flowchart of methods and summary of main findings.** (A) The flowchart gives an overview of the main steps in the analysis of the transcriptomics data. (B) The Venn diagram gives a summary and comparison of the important pathways that were found to be dysregulated in the MPTP mouse SNpc after a single dose and after 14 days of exposure and those that were dysregulated in the SNpc from human PD patients.